N° Order :

N° Serial :

People's Democratic Republic of Algeria

Ministry of Higher Education and Scientific Research

University of Echahid Hamma Lakhdar-El OUED

Faculty of Natural and Life Sciences

Department of Cellular and Molecular Biology

END OF STUDY Dissertation

With a view to obtaining the Academic Master's degree

Subject: Biological Sciences

Specialty: Applied toxicology

THEME

Comprehensive Assessment of Medicinal Plants for Anticancer Properties: In Vitro Assays, ADMET Modeling, Molecular Docking , Analysis, and Molecular Dynamics Simulation

Presented by (05 June 2024) :

- ✓ **Ms AIBA Ilham**
- ✓ **Mrs BELLOUL Hadjer**
- ✓ **Ms CHEKIMA Safa**
- ✓ **Ms FERHAT Amira**

Before the jury compsed of:

President: Dr. NADJI Nassima	M.C.B, University of El-Oued.
Examiner: Dr.LAIB Ibtissam	M.C.B, University of El-Oued.
Supervisor: Dr. LANEZ Elhafnaoui.	M.C.A, University of El-Oued.

Academic year: 2023/2024.

Acknowledgements

Firstly, we would like to express our sincere thanks to Almighty ***ALLAH***, who has enlightened us and opened the doors of knowledge, and who has granted us the will and courage necessary to undertake this work.

We extend our deepest gratitude to Professor ***LANEZ Touhami,*** director of the VTRS research laboratory at the University of El Oued, for providing us with all the necessary means and techniques, and also for welcoming us into his laboratory.

We are profoundly grateful to our supervisor, Doctor ***LANEZ Elhafnaoui***, for agreeing to guide this work, and for his generosity, kindness, encouragement, constant support, and trust in us throughout the preparation of this work.

We also thank the engineers at the VTRS laboratory, ***Mr. TELIBA Ali*** and ***Dr. ADIAKA Aicha***, for their valuable support, encouragement, and advice throughout the completion of this work..

Our thanks also extend to all the members of the *VTRS* laboratory, especially the doctoral student ***DJARALLAH Marwa***.

We wish to express our gratitude towards the administrative staff of the Faculty of Natural Sciences and Life, under the direction of the Dean of the faculty, Mr.***ZAATER Abdelmalek,*** as well as the head of the department of molecular and cellular biology, Doctor ***TLILI M. Laid***, and to all the faculty's teaching staff.

Dedication

In the name of Allah, the Most Gracious, the Most Merciful. With His blessings, I dedicate the fruits of this humble effort and work to those who have been the best support in my academic and professional journey.

To my dear parents ***AIBA Said,BEN AMARA Salima***.who instilled in me the love of knowledge and learning, and never hesitated to support and encourage me at every step, thank you for your patience, endurance, and continuous prayers, which have greatly contributed to achieving this success.

To my beloved mother, the source of love and tenderness, I dedicate this achievement to you with all my love and appreciation for the countless sacrifices you have made. You are the secret behind my success and perseverance.

To my beloved father, the rock of safety and my guide in life, you have always been an example of strength and patience. I am grateful to you for everything you have done for me.

To my dear siblings,***Mahmoud,Abdel Razzak,Imad Eddine*** and my dear sister ***Zinab***,who shared in the joy of every success and stood by me in every challenge, you are my pillars of support and a source of inspiration.

To all my family members and faithful friends who supported and stood by me, thank you all for your support and love.

I pray to Allah Almighty to make this work a source of blessings for all of us, and may it benefit everyone who comes across it. May it be a legacy of goodness in our pursuit of knowledge and success.

Dedication

In the name of Allah, the Most Gracious, the Most Merciful, I dedicate this humble work to the memory of my beloved father, ***BELLOUL Saad,*** who was always compassionate and supportive in my life, and whose departure left an indelible mark on my heart.

To my dear father, who was my guide and support in every moment, I express my deep gratitude and immense appreciation for everything you have done for me. I pray that Allah may encompass you with His vast mercy and grant you a place in His spacious gardens.

To my beloved mother, ***HOUIDI Massouda***, who was a source of strength and determination in the absence of my father, I dedicate this work as an expression of my gratitude and deep love for you. I pray that Allah may grant you patience and solace.

To my dear husband, ***DABBAR Omar***, who has been and continues to be a source of inspiration and unwavering support in my life, I pray that Allah may bless us with the continuation of love and understanding, and grant us happiness and contentment.

To my siblings, ***Abdel-Hay*** and ***Abdel-Moneem***, who were a pillar of support for me after the passing of our father, and to my beloved sisters ***Asmaa*** and ***Hanan***, who have always been by my side in every stage of my life, I express my gratitude and appreciation for your limitless support and love.

To all family members and friends who have encouraged and supported me at every moment, I extend to you all the warmest greetings and deepest gratitude.

I pray that Allah may make this work sincerely for His noble countenance, and may it be a provision for me in this life and a good deed in the Hereafter, and may He have mercy on my parents and grant them a place in His spacious gardens.

Dedication

In the name of Allah, the Most Gracious, the Most Merciful. With His blessings, I dedicate the fruits of this humble effort and work to those who have been the best support in my academic and professional journey.

To my dear parents ***CHKIMA Laïd*** and ***CHEKIMA Rebah***.who instilled in me the love of knowledge and learning, and never hesitated to support and encourage me at every step, thank you for your patience, endurance, and continuous prayers, which have greatly contributed to achieving this success.

To my beloved mother, the source of love and tenderness, I dedicate this achievement to you with all my love and appreciation for the countless sacrifices you have made. You are the secret behind my success and perseverance.

To my beloved father, the rock of safety and my guide in life, you have always been an example of strength and patience. I am grateful to you for everything you have done for me.

To my dear siblings,***Abdel-wahab,khalifa***,***Badr-eddine,****Rachid* ,and my dear sisters ***Wahiba ,Fatiha,Malika,Khadija***,who shared in the joy of every success and stood by me in every challenge, you are my pillars of support and a source of inspiration.

To all my family members and faithful friends who supported and stood by me, thank you all for your support and love.

I pray to Allah Almighty to make this work a source of blessings for all of us, and may it benefit everyone who comes across it. May it be a legacy of goodness in our pursuit or knowledge and success.

Safa

Dedication

In the name of Allah, the Most Gracious, the Most Merciful. With His blessings, I dedicate the fruits of this humble effort and work to those who have been the best support in my academic and professional journey.

To my dear parents ***FERHAT abd elmadjid,FERHAT Sakina***.who instilled in me the love of knowledge and learning, and never hesitated to support and encourage me at every step, thank you for your patience, endurance, and continuous prayers, which have greatly contributed to achieving this success.

To my beloved mother, the source of love and tenderness, I dedicate this achievement to you with all my love and appreciation for the countless sacrifices you have made. You are the secret behind my success and perseverance.

To my beloved father, the rock of safety and my guide in life, you have always been an example of strength and patience. I am grateful to you for everything you have done for me.

To my dear siblings,***Abd elkarim Hocine Hadj elbachir,*** and my dear sisters ***Yasmina*** and ***Zinab***,who shared in the joy of every success and stood by me in every challenge, you are my pillars of support and a source of inspiration.

To all my family members and faithful friends who supported and stood by me,s thank you all for your support and love.

I pray to Allah Almighty to make this work a source of blessings for all of us, and may it benefit everyone who comes across it. May it be a legacy of goodness in our pursuit of knowledge and success.

Amina

Abstract:

This study examines the biological activity of essential oils extracted from the plant *Origanum Majorana L.*, known for its medicinal properties. A sample was selected from the Akfadou region in the El Oued province. Gas Chromatography-Mass Spectrometry (GC/MS) analysis revealed an essential oil production rate of 1.45%. Purity was confirmed through chromatography, ultraviolet (UV) spectroscopy, and cyclic voltammetry tests. The main objective is to evaluate the anticancer activity of the essential oil of *Origanum Majorana L.* through experimental and computational methods, including theoretical molecular docking.

Origanum Majorana L. plants have a long history of medicinal use, prompting exploration of their therapeutic potentials. This study focuses on evaluating their anticancer properties, which are crucial for developing new treatments. In the experimental analysis, cyclic voltammetry (CV) was used to monitor the anticancer activity of the essential oil using DNA and BSA. UV spectroscopy and circular dichroism were employed to validate the results. The essential oil showed significant anticancer activity with DNA (ΔG = -26.55 kJ/mol) and BSA (ΔG = -30.60 kJ/mol), confirmed by UV spectroscopy and circular dichroism (ΔG DNA = -26.89 kJ/mol and ΔG BSA = -32.39 kJ/mol). Among the compounds of the essential oil identified by GC/MS were santolina triene and sabiene.

In the computational part, we obtained results similar to the experimental part, with the essential oil showing results with DNA (ΔG = -5.569) and BSA (ΔG = -6.479). Among the compounds present at more than 1% is Alpha-pinene.

The essential oil of *Origanum Majorana L.* shows significant anticancer activity, warranting further research into its therapeutic mechanisms and clinical applications. Molecular dynamics simulations (MDS) were conducted for the main compound to show the best IFD score of Trans-thujone in complex with BSA. The primary objective of these MDS efforts was to subject the receptor-ligand complex to physiological conditions, an achievement that is challenging to realize through the limitations of molecular docking.

Keywords: *Origanum Majorana L*, essential oils, DNA, bovine serum albumin (BSA), GC/MS (gas chromatography-mass spectrometry), anticancer activity, cyclic voltammetry (CV), theoretical molecular docking, molecular dynamics simulations (MDS), Alpha-pinene, Trans-thujone.

.

Resume:

Cette étude traite de l'activité biologique des huiles essentielles extraites de la plante *Origanum Majorana L.*, connue pour ses propriétés médicinales. Un échantillon a été prélevé de la région d'Akfadou dans la wilaya d'El Oued. L'analyse par chromatographie en phase gazeuse couplée à la spectrométrie de masse (GC/MS) a révélé une production d'huile essentielle à un taux de 1,45 %. La pureté a été confirmée par des tests de chromatographie, des tests aux rayons ultraviolets et des tests de voltampérométrie cyclique. L'objectif principal est d'évaluer l'activité anticancéreuse de l'huile essentielle *d'Origanum Majorana L.* à travers des méthodes expérimentales et computationnelles, y compris le docking moléculaire théorique.

Les plantes *Origanum Majorana L.* ont une longue histoire d'utilisation médicinale, ce qui pousse à explorer leurs potentiels thérapeutiques. Cette étude se concentre sur l'évaluation de leurs propriétés anticancéreuses, essentielles pour le développement de nouveaux traitements. L'analyse expérimentale a utilisé la voltampérométrie cyclique (CV) pour surveiller l'activité anticancéreuse de l'huile essentielle en utilisant l'ADN et la BSA. L'analyse spectroscopique aux rayons ultraviolets et la dichroïsme circulaire ont été utilisées pour valider les résultats. L'huile essentielle a montré une activité anticancéreuse significative avec l'ADN (ΔG = -26,55 kJ/mol) et la BSA (ΔG = -30,60 kJ/mol), confirmée par l'analyse spectroscopique aux rayons ultraviolets et la dichroïsme circulaire (ΔG ADN = -26,89 kJ/mol et ΔG BSA = -32,39 kJ/mol). Parmi les composés de l'huile essentielle identifiés par (GC/MS) se trouvent le santolina triene et le sabiene.

Dans la partie computationnelle, nous avons obtenu des résultats similaires à la partie expérimentale, avec l'huile essentielle présentant des résultats avec l'ADN (ΔG = -5,569) et la BSA (ΔG = -6,479). Parmi les composés présents à plus de 1 % se trouve l'Alpha-pinène.

L'huile essentielle *d'Origanum Majorana L.* montre une activité anticancéreuse significative, nécessitant des recherches supplémentaires sur ses mécanismes thérapeutiques et ses applications cliniques. Des simulations de dynamique moléculaire (MDS) ont été menées pour le composé principal afin de montrer la meilleure affinité de docking (IFD) du Trans-thujone en complexe avec la BSA. L'objectif principal de ces simulations MDS était de soumettre le complexe récepteur-ligand à des conditions physiologiques, un exploit difficilement réalisable par les limites du docking moléculaire.

Mots-clés : *Origanum Majorana L*, huiles essentielles, ADN, sérum albumine bovine (BSA), GC/MS (chromatographie en phase gazeuse et spectrométrie de masse), activité anticancéreuse, voltampérométrie cyclique (CV), docking moléculaire théorique, simulation de dynamique moléculaire (MDS), Alpha-pinène, Trans-thujone.

ملخص

تتناول هذه الدراسة النشاط البيولوجي للزيوت العطرية المستخرجة من نبات *Origanum Majorana L.*المعروف بخصائصه الطبية. تم اختيار عينة من منطقة أكفادو بإقليم الواد. كشف تحليل قياس الطيف الكتلي للغاز (GC/MS) عن إنتاج زيت أساسي بنسبة 1.45%.تم تأكد من نقاوة عن طريق اختبار كروماتوغرافيا و الاشعة فوق البنفسجية و اختبار تصوير المقطعي الدوري.الهدف الرئيسي هو تقييم النشاط المضاد للسرطان للزيت العطري *Origanum Majorana L.* من خلال الأساليب المختبرية والحسابية، بما في ذلك الالتحام الجزيئي النظري.

تتمتع نباتات *Origanum Majorana L.* بتاريخ طويل من الاستخدام الطبي، مما يدفع إلى استكشاف إمكاناتها العلاجية .تركز هذه الدراسة على تقييم خصائصها المضادة للسرطان، والتي تعتبر ضرورية لتطوير علاجات جديدة.- التحليل المختبري: تم استخدام التصوير المقطعي الدوري (CV) لمراقبة النشاط المضاد للسرطان للزيت العطري باستخدام DNA و .BSAتم استخدام التحليل الطيفي للأشعة فوق البنفسجية وازدواجية اللون الدائرية للتحقق من صحة النتائج.حيث أظهر لنا الزيت العطري نشاطًا كبيرًا مضادًا للسرطان مع الحمض النووي (ΔG = -26.55 كيلو جول/مول (و ΔG = -30.60) BSAكيلو جول/مول(، تم تأكيده بواسطة التحليل الطيفي للأشعة فوق البنفسجية وازدواج اللون الدائري = ΔG DNA) 26.89-كيلو جول/مول ΔG BSA = -32.39 .(كيلوجول/مول).ومن بين مركبات الزيت العطري التي تم تحديده بواسطة .santolina triene,sabiene (GC/MS) في الجزء الحاسوبي سجلنا نتائج متقاربة للجزء المختبري حيث ان حيث أظهرت لنا نتائج الزيت العطري مع الحمض النووي (ΔG = -5.569) و BSA (ΔG = -6.479)، من بين مركبات التي تكون نسبتها أكثر من 1 هي Alpha-pinene يُظهر الزيت العطري *Origanum Majorana L.* نشاطًا كبيرًا مضادًا للسرطان، مما يستدعي إجراء المزيد من الأبحاث حول آلياته العلاجية وتطبيقاته السريرية.تم إجراء تحقيقات محاكاة الديناميكيات الجزيئية (MDS) للمركب الرئيسي لإظهار أفضل درجةIFD ، Trans-thujone، في المجمع مع .BSA كان الهدف الرئيسي لمساعي MDS هذه هو إخضاع مجمع مستقبلات الليجند للظروف الفسيولوجية، وهو إنجاز بعيد المنال من خلال حدود الالتحام الجزيئي .

الكلمات المفتاحية:*Origanum Majorana L*,لزيوت العطرية،الحمض النووي،مصل الألبومين البقري) GC/MS, ,تحليل قياس الطيف الكتلي للغاز, ,(النشاط المضاد للسرطان التصوير المقطعي الدوري (CV),الالتحام الجزيئي النظري محاكاة الديناميكيات الجزيئية-Trans ,Alpha-pinene ,(MDS) thujone,

List of Abbreviations

α: Alpha

β:: Beta

Δ**E** : Change in Energy

ΔG : Change in Gibbs Free Energy

µL : Microliter

µM: Micromolar

A°: Angstrom

Abs: Absorbance

DNA: Deoxyribonucleic Acid

ADMET: Absorption, Distribution, Metabolism, Excretion, and Toxicity

BSA: Bovine Serum Albumin

C: Concentration

C°: Celsius Degrees

GC: Gas Chromatography

CV: Cyclic Voltammongrams

MS: Mass Spectrometry

DMSO: Dimethyl Sulfoxide

EDTA: Ethylene diaminetetraacetic Acid

EO: Essential Oil

HCl: Hydrochloric Acid

K: Binding Constant

KCl: Potassium Chloride

Kg: Kilogram

K2HPO4: Potassium Hydrogen Phosphate

KH2PO4:Potassium Dihydrogen Phosphate

KJ: Kilojoule

KOH: Potassium Hydroxid

M: Mole

MDS: Molecular Dynamics Simulation

Min: Minute

NaCl: Sodium Chloride

NaHCO3: Sodium Bicarbonate

NH4Cl: Ammonium Chloride

PDB: Protein Data Bank

pH: Potential of Hydrogen

SDS: Sodium Dodecyl Sulfate

T°: Temperature

TLR: Red Blood Cell Lysis Solution

TLB: White Blood Cell Lysis Solution

TRIS: Tris(hydroxymethyl)aminomethane

UV: Ultraviolet

V: Volume **Vis**: Visible

VTRS: Valorization and Technology of Saharan Resources

List of Figures

List of Tables

Sommaire

References

General Introduction

General Introduction

The use of medicinal plants to treat diseases dates back thousands of years, and is evidence of the constant pursuit of natural therapeutic solutions. In recent decades, the rise in cancer incidence worldwide has seen an increase in intense research into innovative and effective treatments. Among these treatments, medicinal plants have been increasingly recognized thanks to their potential anti-cancer properties, prompting scientific researchers to carry out extensive scientific investigations with the aim of verifying and exploiting these capabilities (**Newman and Cragg.,2020).** Evaluation of medicinal plants for their anti-cancer properties is a popular topic in research. Scientific research due to the great potential it provides in natural treatments. These studies analyze various aspects related to medicinal plants, including their effect on cancer cells and their mechanisms of action, in addition to evaluating the safety of their use and pharmacokinetic properties.

In vitro analysis involves evaluating the ability of plant compounds to kill cancer cells or inhibit their growth, using a variety of cellular and molecular tests. For example, assays of isolated cancer cells can be used to evaluate the effect of plant compounds on the growth of cancer cells compared to normal cells.

In terms of ADMET modeling, these studies aim to understand how plant compounds affect absorption, distribution, metabolism and excretion and to evaluate their potential safety and effectiveness in the body. This analysis involves determining the physicochemical properties of plant compounds and estimating their potential distribution in tissues and biological fluids.

In molecular docking analysis, chemical interactions between plant compounds and molecular targets in cancer cells are studied, which helps to understand mechanisms of action and choose appropriate targets for treatment.

As for molecular dynamics simulations, they are used to analyze the movement and interaction of plant compounds at the atomic level, providing a deep understanding of their interactions with cancer targets at the molecular level**. (Newman and Cragg.,2020).**

Part I:

Bibliographic synthesis

Chapter I:

Medicinal plants

I. Generalities about medicinal plants

1. Historical Overview of Medicinal Plants

The evolution of medicinal plant usage throughout history reflects a profound interaction between human civilizations and the environment for obtaining food and medicine. This knowledge, transmitted across generations, has played a pivotal role in the development of both traditional and scientific medicine. Recent research highlights the significance of medicinal plants as a crucial pharmaceutical resource across various cultures, and today's scientists face major challenges in assessing the quality and safety of these plants. Preserving historical records on the uses of medicinal plants and enhancing collaboration to utilize these resources in developing health care systems based on natural ingredients is increasingly emphasized in contemporary research **(Jamshidi-Kia *et al*., 2018)**.

On the other hand, a historical review published in "Pharmacogn Rev" indicates that healing with medicinal plants is as old as humanity itself. Human use of nature-derived medicines dates back to ancient times, with documented evidence including written documents, preserved landmarks, and even original botanical medicines. Contemporary sciences have recognized the efficacy of these plants and included them in modern pharmacotherapy, thus enhancing the capability of pharmacists and physicians to address contemporary health challenges **(Biljana Bauer &Petrovska .,2012).**

2. Definition of Medicinal Plant

The term "medicinal plants" refers to a diverse array of plants utilized in herbal therapy, often distinguished by their pharmacological properties. These plants serve as a rich source of active compounds utilized in the development and manufacturing of pharmaceuticals. Furthermore, these plants play a pivotal role in shaping human cultures across epochs and various geographical regions. **(Rasool *et al*.,2012)**.

A medicinal plant is defined as any plant containing, in one or more of its parts, substances that can be utilized for therapeutic purposes or considered as raw materials for semi-synthetic pharmaceutical synthesis. When a plant is classified as medicinal, it signifies that the mentioned plant is beneficial as a medicine, therapeutic agent, or active component in pharmaceutical preparation. Herbal medicines are in high demand in both developed and developing countries for primary healthcare due to their broad spectrum of biological and medicinal activities, high safety margins, and lower costs **(Yudharaj *et al.*, 2016).**

3. Basis of Classification of Medicinal Plants:

Medicinal plants have always played a pivotal role as sources of pharmacologically active compounds. Early humans, driven by instinct, taste, and experience, treated their ailments using

plants, making the history of medicinal plants as long as human history itself. One of the challenges facing the evolution of medicinal plants is their classification. Over the years, taxonomists have developed various methods for plant classification, including morphological, anatomical, and chemical classifications. The first two methods fall under traditional classifications, while the third approach represents a modern approach to plant classification. The concept of classifying medicinal plants based on their chemical nature is not new, but over time, it has faced more limitations than possibilities. This chapter discusses how medicinal plants are classified, how information related to their chemical constituents can be used for classification, the problems associated with classification, and useful applications **(Singh & Geetanjali ,, 2018)**.

4. Source of Medicinal Plants

Medicinal plants can be obtained from two main sources. The first source is wild plants, where numerous species grow in valleys, plains, and forests. This may suffice for some plants, such as the yucca plant, which grows wild in countries in central Africa. The second source for obtaining medicinal plants is through cultivation, where pharmaceutical companies or investment institutions establish specialized farms to produce specific varieties or types needed by the local or international market in specific quantities **.(Jamshidi-Kia *et al* .,2017)**

II. Studied plants

1. Origanum Majorana L

1.1. Definition of *Origanum Majorana L*

The name *Origanum* originates from the Greek words "oros," meaning mountain, and "gonos," meaning brightness, thus it became known for its delightful presence in mountainous regions around the Mediterranean basin. **(Prena & Neeru 2015)**. *Origanum Majorana L*, commonly known as Majorana, is a perennial herb. **(VagiE *et al*., 2002)** .It is distinguished taxonomically and morphologically, with forty-nine classifications divided into subgroups distributed around the Mediterranean Sea. This herb is widely known as Marjoram and is native to Anatolia (Turkey) and nearby regions, and it is also found in parts of the Mediterranean region, especially Egypt . **(Novak *et al* ., 2002)**. Marjoram was initially used by Hippocrates as an antiseptic agent. It is an effective remedy for respiratory infections, coughs, and throat inflammation**. (BremnessL., 1994.) (Yazdanparast *et al*., 2008)**

1.2. Classifiction

Table 1: Classification of *Origanum Majorana L* plant

Species	***Majorana L***
Type	*Origamum*
Family	Lamiaceae
Order	Lamiales
Class	Mangnoliopsida
Branch	Mangnoliophyta
Reign	Plants

Picture 1: Photography of *Origanum Majorana L*

1.3. Geographic Distribution of *Origanum Majorana L*

Origanum Majorana L., also known as Marjoram, is native to Turkey and Cyprus and has spread from there to countries around the Mediterranean Sea basin (such as Lebanon), Iran, North America, the Arabian Peninsula, and India. It grows on sunny slopes in meadows, fields, and rocky lands in various climates. It is extensively cultivated in the southern regions of Saudi Arabia **.**

1.4. Previous studies on plants of *Origanum Majorana L*

The chemical composition and mineral elements of marjoram leaves were estimated, and the percentage content of moisture, protein, fat, ash, and carbohydrates was (5.7/66.3/18.7/84/6.6), while the element concentrations were 0.01/0.65.1/0.039/0.49 parts per million. Respectively, the effective mineral aggregates (Ba. Fe. K. Co. Na) were identified by conducting qualitative tests on the aqueous and alcoholic herb extracts, as it was observed that they contain tannins, phenols, flavonoids, soaps, carbohydrates, and alkaloids. Physical and chemical tests were studied, such as burning and solubility, as it was observed that they partially

dissolved inpolar solvents. Completely in non-polar solvents. (http://Imagerie-puces-a-cellules.univ)The effect of ground herb leaves as a preservative was studied for beef at concentrations of (105) stored by refrigeration at 5 degrees Celsius for a period of 7-100 days. The changes occurring in the pieces of meat were followed by estimating the peroxide number, where the results showed a decrease in its value in samples treated with powdered herb leaves. In comparison with the fresh sample during the storage period, its effect on the logarithm of the numbers of kidney bacteria and coliform bacteria present in the meat at the same storage period and previous concentrations was also studied. The results showed that the herb has a role in reducing the numbers of microorganisms in samples of minced meat, as well as having antioxidant activity by prolonging the meat life of the pieces. the meat .

(Charai .,1996).

III. Chemical and physical studies

1. Generalities about essential oils

Essential oils are highly concentrated plant extracts known for their aromatic properties and cold pressing, therapeutic benefits. They are obtained through processes like distillation or capturing the essence of the plant's fragrance and medicinal properties. These oils have been used for centuries in various cultures for their healing properties, such as reducing stress, research has also demonstrated their improving mood, and promoting relaxation. Scientific inflammatory, and antioxidant effects-potential health benefits, including antimicrobial, anti. **(Worwood, 2016)**

2. Hydrodistillation extraction :

Hydrodistillation is a widely-used method for extracting essential oils from plant materials. In this process, the plant material is placed in a distillation vessel, either directly submerged in water or contained within a mesh container to prevent contact with the vessel walls. The vessel, typically made of non-corrosive materials like copper or glass, is heated, usually by a fire or an electric heater. Hydrodistillation is particularly suitable for plants with high oil content in parts such as roots, leaves, fruits, and certain flowers **(Baser & Buchbauer, 2010).**

3. Gas Chromatography-Mass Spectrometry (GC/MS) analysis of essential oils

The combination of gas chromatography and mass spectrometry allows for the simultaneous separation and analysis of components.

Different types of the compound mixture. The important development of mass spectrometry in identifying and discovering the components of perfumes and essential oils was made possible by linking Gas chromatography and mass spectrometry, as it became possible to obtain a

clear mass spectrum for quantities A small amount of matter, ranging from micrograms to nanograms, is also possible thanks to this important innovation in mass spectrometry.

It has become the most sensitive technique for obtaining important data regarding the structure of an unknown organic compound **(Vagi et al., 2005)**

Among the most widely used ionization methods in analyzing mixtures of compounds, we mention:

- Negative Chimique Ionisation(ICN)
- Negative Chimique Ionisation (ICP)
- Electron impact ionization : Ionisation Impact Electronic(IE).

The components of the mixture injected into the device pass through the column in their gaseous state at different speeds and are held with retention times.

TR different according to their solubility in the stationary phase, then the components of the complex mixture are separated inside the chromatography column.

In the ionization chamber, you are bombarded with a stream or flood of electrons with an energy of about 70ev. This energy causes: different molecules are displaced or broken (fragmentation), then the resulting positive ions head towards the analyzer (Magnétique or Quadripôle)the obtained stray current is transformed into a

An electron that swells and expands to give a mass spectrum. **(Chamblee, 1997).**

4. Analysis of Essential Oils by UV-VIS Spectroscopy:

Recent studies have proven the important role of alternative medicine in medical applications, which prompted us to conduct a simple spectroscopic study of some of the natural oils used. The study highlighted the UV-VIS analysis technique as a non-destructive and rapid method to determine the absorption spectrum of some natural oils known for their medicinal purposes. **(Numan *et al*., 2024).**

The UV-VIS analysis technique depends on measuring the amount of light absorbed by a specific sample in the visible and ultraviolet spectrum range. This is done by directing a beam of light through the sample, and then measuring the amount of light absorbed by the sample at each wavelength. The absorption strength of a sample depends on the concentration of compounds present in it and the wavelength used. Based on the measurements obtained, the composition of the sample can be determined and the concentrations of various compounds in it can be estimated.

5. Electrochemical technology :

Oils involves the use of various electrochemical techniques to Electrochemical analy-

sis of assess the composition, quality, and properties of oils. These techniques utilize the electr cal properties of oil constituents to provide valuable insights into their chemical makeup. One common electrochemical method is cyclic voltammetry, which measures the current response as a function of applied voltage to study the redox behavior of oil components. Another technique is electrochemical impedance spectroscopy, which characterizes the electrical response of oil samples to alternating current across a range of frequencies, providing information about their conductivity and capacitance properties. Electrochemical analysis offers several advantages, including high sensitivity, rapid analysis times, and the ability to perform measurements directly in the oil sample without extensive sample preparation. situ monitoring of oil -Additionally, electrochemical techniques can be employed for in properties, making them valuable tools for quality control and process optimization in industries such as food, pharmaceuticals, and cosmetics **(Brett, 2012).**

Chapter II:

Cancer

1. A brief history of cancer

Cancer has a rich historical background that spans thousands of years. The earliest documented references to cancer date back to ancient Egypt, where evidence of tumors and growths were found in skeletal remains dating back to around 3000 BCE. Ancient Egyptian texts, including the Edwin Smith Papyrus and the Ebers Papyrus, describe cases that may have been cancer and suggest early attempts at understanding and treating the disease. Throughout history, cancer has been described and treated in various ways across different cultures and civilizations. In ancient Greece, the physician Hippocrates coined the term "carcinos" (meaning crab) to describe tumors, and he proposed the theory that cancer arises from an excess of black bile. This theory of the four humors, including black bile, yellow bile, phlegm, and blood, influenced medical thought for centuries. The Renaissance period brought about advancements in anatomy and pathology, leading to a deeper understanding of cancer as a disease of abnormal tissue growth. In the 19th century, with the advent of microscopy and cellular pathology, German pathologist Rudolf Virchow proposed the theory that cancer originates from cells, laying the groundwork for modern oncology. The 20th century witnessed significant progress in cancer research and treatment. Discoveries such as the identification of carcinogens, the role of genetic mutations in cancer development, and the development of chemotherapy and radiation therapy revolutionized cancer care. Today, ongoing research continues to expand our understanding of cancer biology, leading to the development of targeted therapies, immunotherapies, and precision medicine approaches . **(Mukherjee, 2011).**

2. Definition of cancer

Cancer is a complex and heterogeneous group of diseases characterized by uncontrolled growth and spread of abnormal cells in the body. These abnormal cells, known as cancer cells, have the ability to invade surrounding tissues and organs, disrupting their normal function. Cancer can arise in virtually any part of the body and can manifest in various forms, including solid tumors (such as those found in the breast, lung, or colon) and

Hematological malignancies (such as leukemia and lymphoma). The development of cancer is often multifactorial and involves genetic, environmental, and lifestyle factors. Genetic mutations can disrupt the normal regulation of cell growth and division, leading to the formation of cancerous cells. Environmental factors such as exposure to carcinogens (such as tobacco smoke, ultraviolet radiation, and certain chemicals) can increase the risk of developing cancer. Additionally, lifestyle factors such as diet, physical activity, and tobacco use play a significant role in cancer

Development. The hallmark characteristics of cancer include uncontrolled cell proliferation, evasion of cell death (apoptosis), sustained angiogenesis (formation of new blood vessels), tissue invasion, and metastasis (spread to distant organs). Cancer is a leading cause of morbidity and mortality worldwide, accounting for millions of deaths each year **(ACS, 2021)**

3. Causes of cancer

Cancer develops due to abnormal genetic changes in the body's cells, leading to uncontrolled and irregular cell growth. These alterations can be induced by environmental factors such as smoking and exposure to radiation, coupled with genetic influences that may elevate the risk of cancer. Numerous studies underscore the significance of a healthy lifestyle and dietary choices in cancer prevention. **(WHO, 2020)**

4. Types of cancer

4.1. Breast cancer

Is a type of cancer that originates in the mammary tissue. It can start in one or both breasts. Breast cancer usually occurs in women, but it can also affect men. Although most breast lumps are benign and noncancerous, some benign tumors can increase your risk of developing breast cancer in the future. Any breast changes or lumps should be examined by a doctor to determine their nature and whether they are serious or not. **(Cossis et al .,2020).**

4.2. Lung Cancer

Lung cancer develops in the tissues of the lungs, usually in the cells lining the air passages. Smoking is the leading cause of lung cancer, but non-smokers can also develop it due to exposure to secondhand smoke, radon gas, or other environmental factors. **(ACS, 2021)**

4.3. Colon cancer

Is a disease of the lining, which lines the inside of the colon or the rectum for rectal cancer. Colorectal tumors generally develop from the lining that covers the walls of the colon and rectum.Colorectal cancer takes several years to develop, about 9 to 10 years. It forms from the transformation of a benign tumor, a polyp (fleshy outgrowth) that appears on the mucosa. **(Adrouny *et al* .,2002.)**

4.4. Prostate cancer

Is a type of cancer that develops in the prostate, a gland in the male reproductive system that plays a key role in producing prostatic fluid, which contributes to the survival, maturation, and movement of sperm. The function of the prostate depends on testosterone, a hormone produced by the testes, and its development begins at puberty. As men age, the prostate may be prone to health issues such as benign prostatic hyperplasia, which can lead to difficulty urinating, and prostate cancer, the most common cancer among men. **(Rawla &Prashanth .,2019).**

4.5. Skin Cancer (Melanoma):

Skin cancer, including melanoma, develops in the cells of the skin. Risk factors include sun exposure, indoor tanning, fair skin, history of sunburns, and family history of skin cancer. Early detection and treatment are crucial for preventing the spread of melanoma.**(Boukamp &Petra .,2005).**

5. Cancer diagnosis

The malignant transformation of cancer cells causes cancer as a result of the long-term accumulation of genes and genetic factors, known as epigenetic events. Early diagnosis of these cell transformations is vital to improve the prognosis of disease and cancer. Cancer screening methods include:

5.1. Histological Methods

Histological methods rely on microscopy to carefully examine tissues, and rely on clincal data and investigation. These methods are considered the most valuable for accurate diagnosis, as the diagnosis is made by comparing cytological features between benign and malignant tumors. Benign tumors are defined by their similarity to normal tissue and their inability to invade, while malignant tumors are defined by the presence of dedifferentiation of cells, and may be accompanied by invasion and cytoskeletal deformity.

5.2. Cytological Methods:

These methods for diagnoss consist of study of cells shed off into body cavities and study of cell by puttng afne neede introduced under vacuum into the eson (fine needle aspration cytology FNAC).

5.3. Molecular Diagnostic Technique:

The group of molecular biologic methods in the tumour diagnostic laboratory are a variety of DNA/RNAbased molecular technque in which the DNA/RNA are extracted from the cell and then analysed.the molecuar methods in tumour dagnosis can be appliedin hematoogicas well as

non-hematologcmalignancies by:

-Analysis of molecular cytogenetc abnormalities.

-Mutatonal analysis.

-Antigen receptor gene rearrangement and

-By study of the oncogenic viruses at molecular level.**(Harika *et al* .,2015).**

6. Cancer treatment

Encompasses a range of therapeutic modalities aimed at controlling or eliminating cancerous cells in the body. These treatments may include surgery, chemotherapy, radiation therapy, immunotherapy, targeted therapy, hormone therapy, and stem cell transplant. The choice of treatment depends on factors such as the type and stage of cancer, as well as the patient's overall health and preferences. Advances in cancer research have led to the development of innovative treatments and personalized medicine approaches, improving outcomes for many cancer patients."**(ACS., 2021).**

7. DNA: A Molecular Target of Anticancer Drugs

The primary intracellular target of anticancer drugs is DNA. Newer, more effective drugs that target DNA, damage cancer cells, inhibit cell division, or even kill them, could speed up the drug discovery and development process. It has thus been found useful to study the interaction of metallic compounds with DNA to better understand their pharmacological properties. As a result, complex mechanisms that explain the processes ranging from the production of lesions in DNA to cell death are now available, opening promising prospects for the development of new, more selective, and more effective anti-tumor agents. **(Karoui *et al*., 2022)**.

8. The role of bovine serum albumin (BSA) in cancer treatment:

Nanotechnology is advancing at a great pace and is being used to treat, prevent and diagnose many diseases. Natural agents (drugs/polymers) are believed to be preferable because they have greater biological safety, biodegradability and negligible toxicity. Therefore, they are being investigated to make nanomaterials safer and eligible for clinical translation. Albumin, a globular protein, is important in this regard due to its properties such as biocompatibility, biodegradability, immunogenicity, non-toxicity, water solubility, cost-effectiveness, and tumor targeting ability. Albumin was previously used as a plasma volume expander but has now emerged as a potential drug carrier and delivery vehicle. Albumin finds many applications such as therapeutic agents, biosensors, contrast agents, implants, etc. Albumin nanoparticles have been developed to target cancer**(Maurya *et al* .,2021).**.

9. Essential oils ans cancer

There is no research that proves that essential oils have a significant ability to treat cancer, so you cannot Let's say that 100 percent, despite the history of natural oils, a lot of studies have been done that... Conducted on the effect of aromatherapy. Chemical treatments greatly affect the body, making it feel a lot of fatigue, pain, nausea, constipation, and diarrhea. They also make the skin dry, but essential oils have the ability to help with these diseases, and they can also be One of the factors that help fight cancer cells. **(De Sousa *et al* .,2015).**

Bibliographic References

- Adrouny, A. R. (2002). Understanding colon cancer. Univ. Press of Mississippi.
- American Cancer Society. (2021)
- American Cancer Society. Cancer Treatment
- Baser, K. H., & Buchbauer, G. (2010). *Handbook of Essential Oils: Science, Technology, and Applications*. CRC Press.
- Biljana Bauer Petrovska,(2012) "Historical review of medicinal plants' usage, *Pharmacognosy reviews* 6.11 ,1)
- Boukamp, P. (2005). Non-melanoma skin cancer: what drives tumor development and progression?. Carcinogenesis, 26(10), 1657-1667.
- BremnessL(1994), The Complete Book of Herbs, A Practical Guide to Growing and Using Herbs, Studio, Seattle Goodwill, WA, USA, .
- Brett, C. M. A., & Brett, A. M. O. (Eds.). (2012). *Electroanalysis in Biomedical and Pharmaceutical Sciences: Voltammetry, Amperometry, Biosensors, Applications*. John Wiley & Sons.
- Chamblee, T. S., Karelitz, R. L., Radford, T., & Clark Jr, B. C. (1997). Identification of sesquiterpenes in citrus essential oils by cryofocusing GC/FT-IR. *Journal of Essential Oil Research*, 9(2), 127-132.
- Charai, M., Mosaddak, M., & Faid, M. (1996). Chemical composition and antimicrobial activities of two aromatic plants: Origanum majorana L. and O. compactum Benth. *Journal of Essential Oil Research*, 8(6), 657-664.
- Cossis, K. R., Mahan, T., Dennin Johney, S., & Lowentritt, B. (2020). Testicular Cancer. *In Chemotherapy and Immunotherapy in Urologic Oncology: A Guide for the Advanced Practice Provider* (pp. 279-293). Cham: Springer International Publishing.
- De Sousa, Damião Pergentino, ed. *Bioactive essential oils and cancer*. Springer, (2015).
- Harika, V., Vanitha, K., Harika, Y., Yamini, J., & Sravani, T. (2015). Diagnosis of cancer. *International Journal of Research in Pharmacy and Chemistry*, 5(2), 299-306. ISSN: 2231-2781. Retrieved from http://www.ijrpc.com
- Jamshidi-Kia, Fatemeh, Zahra Lorigooini, and Hossein Amini-Khoei. "Medicinal plants: Past history and future perspective." *Journal of herbmed pharmacology* 7.1 (2017): 1-7.
- Karoui, A., Cheriet, S., Meissa, A., & Ghezal, C. (2022). *Evaluation de la quantité de la nicotine et étude des activités biologiques de trois formes de tabac: tabac commercial, tabac traditionnel et Nicotiana tabacum*. 35-37.
- Jamshidi-Kia, F., Lorigooini, Z., & Amini-Khoei, H. (2017). Medicinal plants: Past histo-

ry and future perspective. *Journal of herbmed pharmacology*, 7(1), 1-7.

- Mukherjee, S. (2011). The Emperor of All Maladies: *A Biography of Cancer*. Scribner.
- Newman, D. J., & Cragg, J. M. (2020). Natural products as sources of new medicines during nearly four decades from 01/1981 to 09/2019. *Journal of Natural Products*, 83(3), 770-803
- Novak, J., Langbehn, J., Pank, F., & Franz, C. M. (2002). Essential oil compounds in a historical sample of marjoram (Origanum majorana L., Lamiaceae). *Flavour and fragrance journal*, 17(3), 175-180.
- Numan, N. H., Hussein, K., Sadkhan, A. K., & AL-Nuwab, M. A. (2024). Characterization of Some Natural Oils Used for Medical Purposes by Ultraviolet – Visible spectroscopy.

  University of Technology Journal, 105(52), 109-119.
- Prena and Neeru Vasudeva, Origanum majorana L. -Phyto-pharmacological review Indian Journal of natural products and Ressourcesm 2015.
- Priyadarshini, R. (2016). Importance and Uses of Medicinal Plants – An Overview. **International Journal of Preclinical & Pharmaceutical Research**, 7(2), 67-73. e-ISSN: 2249-7552. Print ISSN: 2229-7502. Available at: www.preclinicaljournal.com.
- Rasool Hassan, B. A. "Medicinal plants (importance and uses)." *Pharmaceut Anal Acta* 3.10 (2012): 2153-435.
- Rawla, Prashanth. "Epidemiology of prostate cancer." *World journal of oncology* 10.2 (2019): 63.
- Singh, R., & Geetanjali. (2018). Chemotaxonomy of Medicinal Plants: Possibilities and Limitations. In Natural Products and Drug Discovery: An Integrated Approach (pp. 119-136)
- Vagi, E., Rapavi, E., Hadolin, M., Vasarhelyine Peredi, K., Balazs, A., Blazovics, A., & Simandi, B. (2005). Phenolic and triterpenoid antioxidants from Origanum majorana L. herb and extracts obtained with different solvents. *Journal of agricultural and food chemistry*, 53(1), 17-21.
- Vagi, E., Simándi, B., Daood, H. G., Deak, A., & Sawinsky, J. (2002). Recovery of pigments from Origanum majorana L. by extraction with supercritical carbon dioxide. *Journal of agricultural and food chemistry*, 50(8), 2297-2301.
- World Health Organization. (2020). Cancer
- Worwood, V. A. (2016). The Complete Book of *Essential Oils and Aromatherapy*
- Yazdanparast, R., & Shahriyary, L. (2008). Comparative effects of Artemisia dracuncu-

lus, Satureja hortensis and Origanum majorana on inhibition of blood platelet adhesion, aggregation and secretion. *Vascular pharmacology*, 48(1), 32-37.

- Yudharaj, P., Shankar, M., Sowjanya, R., Sireesha, B., Ashok Naik, E., & Jasmine Priyadarshini, R. (2016). *Importance and Uses of Medicinal Plants – An Overview. International Journal of Preclinical & Pharmaceutical Research,* 7(2), 67-73.

Part II:

EXPERIMENTAL

CHAPTER 1:

Materials and methods

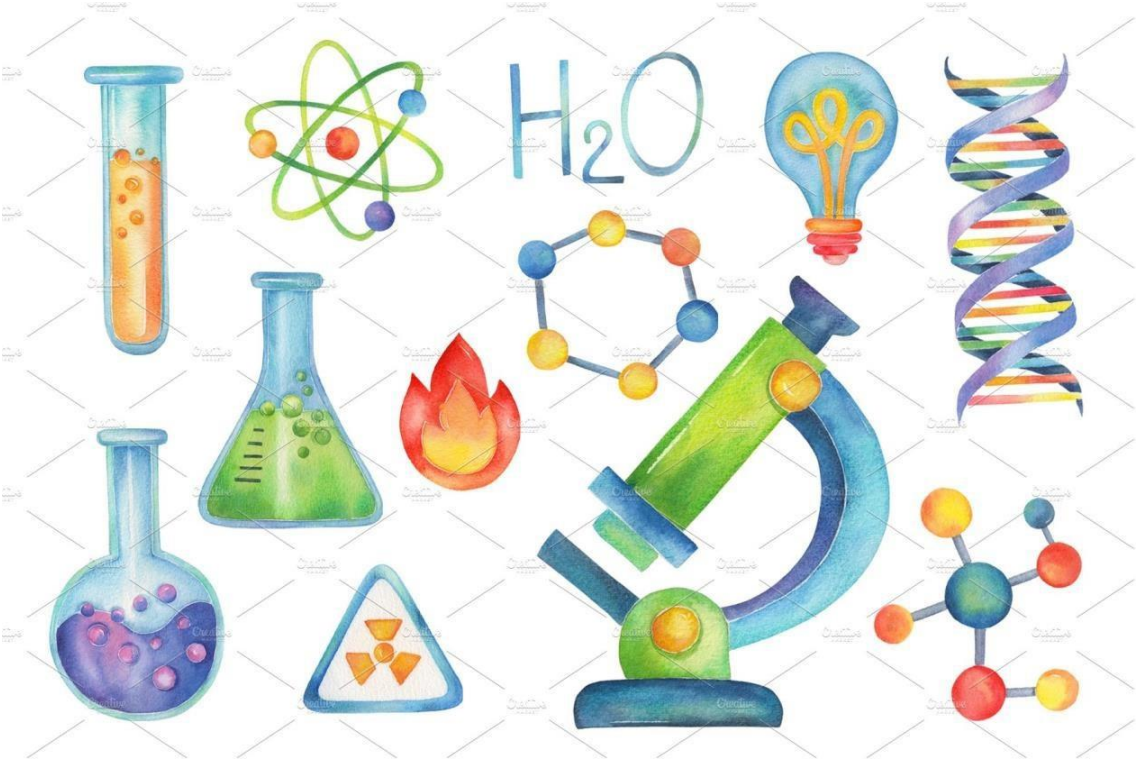

1. Introduction

This study was conducted collaboratively between two specialized laboratories: the Valorisation and Technology of the Saharian Resources Laboratory (VTRS) at the Faculty of Exact Sciences, Department of Chemistry, University of El Oued, and the Centre de Recherche Scientifique et Technique en Analyses Physico-Chimique (CRAPC) in Ouargla, Algeria. The VTRS lab facilitated essential oil extraction, conducted *in vitro* and *in-silico* assays. Meanwhile, CRAPC handled the precise GC/MS analysis of the extracted oils. This collaborative effort ensured thorough and accurate experimentation, combining expertise and resources from both institutions.

2. Plant Material

2.1. Origanum Majorana L

The *Origanum Majorana L* plant was harvested at different time intervals extending from March 2023 to April 2023 in a desert forest area in southeastern Algeria, specifically in Akfadou region in El Oued province. This region is characterized by the following specifications:

- Geographic Coordinates: Longitude 67°6' East, Latitude 33° North.
- Elevation above Sea Level: 58 meters.
- Distance from Sea Level: 300 kilometres.
- Bioclimatic Characterization: Desert.

3. Chemicals and reagents

Bovine Serum Albumin (BSA):

A solution of BSA, obtained from the educational laboratory of the biology faculty, was used as is without purification to achieve a concentration of 250 mg/50 ml in a phosphate saline buffer solution (pH = 6.33).

DNA Extraction Reagents:

Blood: Chicken blood was collected and kept directly on ice for DNA extraction.

Red Blood Cell Lysis Buffer (TLR): Prepared by mixing EDTA (0.1mM), $NaHCO_3$ (12mM), NH_4Cl (155mM) in distilled water.

White Blood Cell Lysis Buffer (TLB): Prepared by mixing NaCl (50mM), EDTA (100mM), Tris (10mM) at pH=7.42.

SDS Solution (20%): Prepared by mixing 2mg of sodium dodecyl sulphate in 10ml of distilled water.

Saturated NaCl Solution: Prepared by mixing 7g of sodium chloride in 10ml of distilled water.

Phosphate Buffer Solution:

The phosphate buffer saline solution was meticulously prepared using sodium dihydrogen phosphate and disodium hydrogen phosphate (Sigma Aldrich) in conjunction with double- distilled water and KCl. The pH was meticulously maintained at 6.4 through the utilization of this phosphate buffer.

4. Materials and Methods

4.1. Essential Oils Extraction

4.1.1. Apparatus:

The essential oil extraction process required the use of specialized equipment to ensure accuracy and efficiency. In this study, the following apparatus was utilized:

- ✓ Adventurer – Pro AV53 sensitive balance
- ✓ Heating flask
- ✓ Refrigerant
- ✓ Clevenger apparatus
- ✓ Separating funnel
- ✓ Rotary evaporator

The Clevenger apparatus, a key component in the extraction process, is depicted in Figure 2

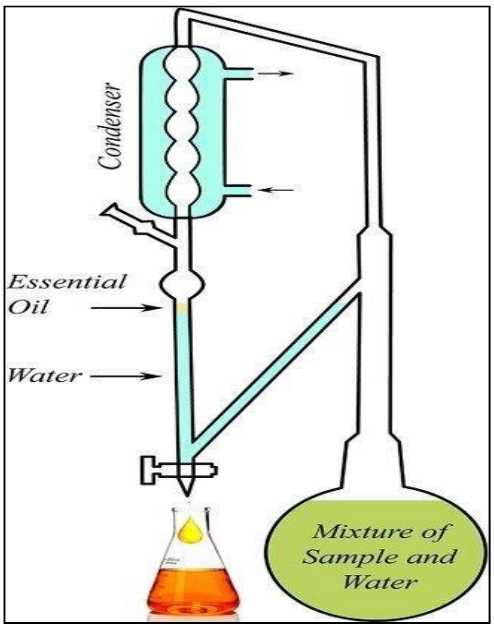

Figure2. Schematic representation of the Clevenger apparatus used in the essential oil extraction process **(Biswa *et al*., 2023)**

4.1.2. Procedure:

The procedure for essential oil extraction involved a series of meticulous steps to ensure optimal results. The extraction process was conducted as follows:

- ✓ Cleaning of the plant sample to remove any impurities.
- ✓ Weighing the plant sample to a quantity of 100 g using a sensitive balance.
- ✓ Washing the plant sample with water to prevent burning, followed by placement in a heating flask.
- ✓ Addition of small pieces of boiling regulator to the flask.
- ✓ Direct heating of the mixture at a temperature of 100 degrees Celsius for three and a half hours.
- ✓ Conducting the steam distillation process and subsequent separation of oil and water phases using liquid-liquid separation with diethyl ether.
- ✓ Drying of the organic oily phase with anhydrous sodium sulphate.
- ✓ Filtration of the dried oil phase through filter paper to remove diethyl ether particles.
- ✓ Evaporation of the filtered oil phase using a rotary evaporator to remove any remaining organic solvent.
- ✓ Storage of the obtained essential oil in small brown bottles and refrigeration at a tem-

perature of 5°C.

4.2. Yield of Essential Oil Extraction

Two distinct methodologies are commonly employed to ascertain the yield of essential oil extraction, each offering unique perspectives on the efficiency of the process.

4.2.1. Volumetric Yield - Mass-based (Naima et al., 2019)

This method entails an assessment of the mass of the utilized plant material intended for essential oil extraction, juxtaposed against the volume of the resultant oil. The yield is then computed utilizing the following

Equation 1:

$$R_{EO} = \frac{V_{EO}\,(ml)}{m_0\,(g)} \times 100 \quad \text{..... (1)}$$

Where: R_{EO}: Essential oil yield, m_0: Mass of the utilized plant sample, V_{EO}: Volume of the extracted essential oil

4.2.2. Mass-based Yield - Mass-based (Larbi et al., 2018)

Alternatively, the essential oil extraction yield is defined as the quotient of the mass of the extracted essential oil and the mass of the plant material utilized. This yield is calculated using

Equation 2:

$$R_{EO} = \frac{m_{EO}\,(g)}{m\,(g)} \times 100 \quad \text{.....(2)}$$

Where: R_{EO}: Essential oil yield, m_0: Mass of the utilized plant sample, m_{EO}: Mass of the extracted essential oil

These methodologies have been systematically applied to derive essential oil yields for all examined plant specimens.

4.3. Characterization of Essential Oils:

The characterization of essential oils comprises two fundamental components: physico-chemical properties and Gas Chromatography-Mass Spectrometry (GC/MS) analysis.

4.3.1. Physicochemical Properties:

Here, we delve into the fundamental traits of essential oils, including their relative density,

acidity, ester content, and refractive index. These properties offer valuable insights into the composition and behavior of essential oils, helping us understand their chemical makeup and how they interact with their environment **(Atti-Santos et al., 2005).**

- *Relative Density (AFNOR NF T75-111 Standard):*

At 20°C, 1 mL of the essential oil is measured using a pipette, and its mass is then determined. The procedure is repeated for distilled water, and density is calculated using the following Equation 3 **(Valarezo et al., 2015):**

$$d = \frac{m_{EO}}{m_{H\,O}} \quad \text{…….. (3)}$$

- *Acidity Index (AFNOR NF T75-111 Standard)*:

To determine the acid value, representing the concentration of free acids in 1 g of the essential oil, a titration method with potassium hydroxide (KOH) solution is employed **(Sahoo et al., 2007)**.

Initially, a small aliquot (0.5 mL) of the essential oil is mixed with 2 to 3 drops of phenolphthalein indicator in a small vessel. Subsequently, titration is performed with 0.5 N KOH solution until the appearance of a faint pink colour, indicating complete neutralization of the acids. The acid value is then calculated using the following Equation 4.

$$I_a = \frac{56.11 \times V \times C}{m} \quad \text{…….. (4)}$$

Where: V: the volume of the KOH solution, C: Concentration of KOH, m: the mass of the essential oil

- *Ester Index (AFNOR NF T75-111 Standard):*

The determination of free acids resulting from ester hydrolysis within the essential oil involves a titration process utilizing 0.5 N potassium hydroxide (KOH) solution **(Alajtal et al., 2018).**

- Begin by placing 0.5 mL of the essential oil into a small vessel.
- Add 1 mL of 0.5 N potassium hydroxide (KOH) solution to the vessel to initiate the titration process.

- Place the mixture in a gas-evacuated water bath for a specified duration to facilitate reaction.
- After cooling, introduce 0.5 mL of distilled water and add 3 drops of phenolphthalein indicator to the mixture.
- Titrate the excess potassium hydroxide (KOH) using 0.5 N hydrochloric acid (HCl) until a colour change is observed, indicating neutralization.
- Quantify the volume of hydrochloric acid (HCl) required to neutralize the excess potassium hydroxide (KOH).
- Calculate the ester content using the following Equation 5:

$$I_e = \frac{2805}{m}(V_0 - V_1) - I_a \qquad \text{…….. (5)}$$

Where: V_0 (ml): Volume of hydrochloric acid (HCl) without essential oil, V_1 (ml): Volume of hydrochloric acid (HCl) in the presence of essential oil, I_a: Acid value, I_e: Ester value and m: Mass of the essential oil sample.

➢ *Refractive Index (AFNOR NF T75-111 Standard):*

The refractive index of an essential oil is defined as the ratio between the sine of the angle of incidence and the sine of the angle of refraction of a light ray, with a specific wavelength, transitioning from air into the essential oil, while the latter is maintained at a constant temperature **(Singh, 2002)**

The refractive index of the essential oil is directly measured using a refractometer at a reference temperature 20°C.

4.3.2. Gas Chromatography-Mass Spectrometry (GC/MS) analysis:

The coupling (GC/MS) technique stands as the most frequently employed method within the field of essential oils, facilitating the concurrent separation, identification, and quantitative measurement of the various constituents present in extracted oils.

➢ Principle:

The principle is founded on the varying affinities of compounds within the mixture towards two phases: a stationary phase and a mobile phase. This technique relies on the distribution of constituents between a stationary phase and a gas phase. The stationary phase comprises a silicone-based liquid that permeates an inert and granular solid material, housed within a typically coiled steel or glass column measuring 1 to 3 meters in length and 2 to 4 millimetres in diameter. The mobile phase consists of an inert carrier gas such as nitrogen, helium, or argon. The

column is maintained at a high temperature via a furnace. Under the influence of temperature, constituents vaporize and become separable. The basis of separation lies in the discrepancy of partition coefficients of volatile compounds between the stationery and gas phases. A detection system generates a signal at the exit of each molecule from the column, manifesting as the recording of peaks corresponding to each constituent.

Gas chromatography is coupled with a mass spectrometer (MS); this coupling relies on computerized comparison of the spectrum of an unknown peak with one or more reference libraries, enabling its identification.

➢ Apparatus:

The identification of the chemical constituents of our essential oils was performed using a gas chromatographic system (HP 5890-SERIE II) equipped with an HP5 MS capillary column (30 meters in length, 0.25 mm internal diameter, and 0.25 μm film thickness) coupled with a mass spectrometer (HP-MSD 5972).

N_2 was employed as the carrier gas for the analysis of the two essential oils. Spectra were recorded at an emission energy of 70 eV, and spectral analysis of the compounds was conducted by comparison with their counterparts using the WILEY275 **(Chiu et al., 1982; Guinaudeau et al., 1975; Kiryakov, 1968; Shamma, 1972)** spectral librairies.

➢ Procedure:

The carrier gas (N_2) is introduced at a flow rate of 1 mL/min, with the injected volume of the essential oil being 1 μL in split injection. The injector and detector temperatures are set at 250°C and 320°C, respectively. The oven temperature is programmed to initially reach 60°C and held for 8 minutes, then gradually increased to 250°C at a rate of 2°C/min, maintained isothermally at 250°C for 15 minutes, and finally elevated to 300°C at a rate of 10°C/min.

4.4. *In Vitro* Assessment of Anticancer Activity

4.4.1. DNA Extraction:

The isolation of DNA from blood can be achieved using various techniques, different protocols, and a wide range of commercially available kits **(Filote et al., 2022).** The chosen DNA extraction technique should be able to provide pure DNA samples ready for use in studying anticancer activity with essential oils.

In this study, we isolated DNA from chicken blood using salting-out techniques **(Gaaib et al., 2011; Miller et al., 1988)**. The advantage of this technique is that it avoids the use of toxic

and corrosive organic solvents and only utilizes standard chemicals that can be obtained from any commercial supplier, and it does not require specialized equipment or biochemical knowledge **(Nasiri et al., 2005; Rivero et al., 2006).** The DNA purification protocol is based on protein precipitation at high salt concentration. The traditional protocol involves initial cell disruption and digestion with sodium dodecyl sulphate, followed by the addition of high salt concentrations, typically 6 M sodium chloride. The mixture is then centrifuged to allow proteins to precipitate to the bottom, with the supernatant containing the transferred DNA into a new flask. DNA is then precipitated using cold ethanol **(Howe, 1997).** The steps involved in DNA extraction are summarized in Figure 3.

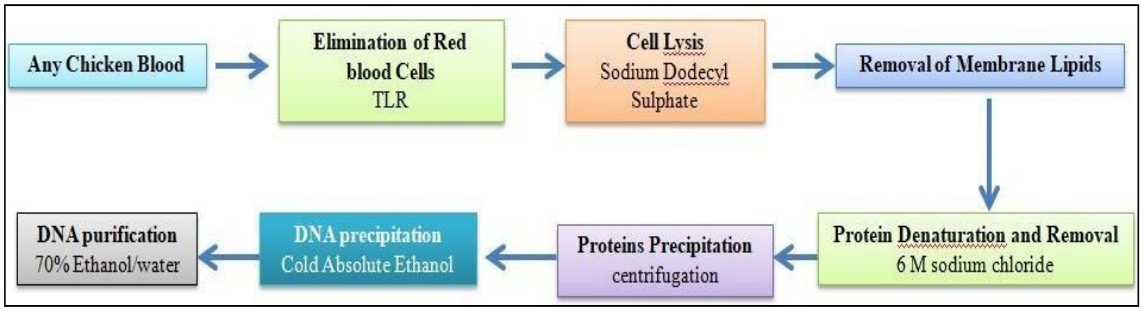

Figure3. Steps Involved in DNA Extraction

✓ *Blood Sample:*

DNA is extracted from chicken blood using salting-out techniques. Chicken blood differs from human blood in that red blood cells are also nucleated and contain much more DNA than non-nucleated mammalian blood. This allows for obtaining chicken DNA in sufficient quantity and quality using relatively simple extraction techniques. Therefore, during DNA purification from chicken blood, there is more DNA material compared to working with human blood **(Ja- vanrouh & Jelokhani-niaraki, 2020)**.

✓ *Blood Collection:*

Samples of chicken blood were collected in blood collection tubes containing EDTA as an anticoagulant and stored at room temperature in microcentrifuge tubes, and extracted on the same working day.

✓ *Extraction Procedure:*

5 ml of whole chicken blood sample is placed in a 20 ml flask, then 10 ml of TLGR (Red Blood Cell Lysis Buffer) was added to the blood and the resulting mixture was cooled in an ice bath for 20 minutes, then centrifuged at 2500 rpm for 15 minutes at room temperature. This step was repeated 3 to 4 times until the red color of the blood disappeared, then the flask was left to dry for 5 minutes.

The white blood cells were removed by adding 2 ml of TLGB buffer and vortexed for 3 minutes. Subsequently, cell lysis was carried out by adding 150 µL of sodium dodecyl sulphate solution and centrifuged at 172 rpm for 90 minutes at 55°C. After centrifugation, 3 ml of 6 M sodium chloride solution was added, and the resulting mixture was vortexed for 6 minutes and then centrifuged at 1300 rpm for 10 minutes. The liquid phase was recovered, and 2 volumes of cold isopropanol were added, followed by centrifugation at 1300 rpm for 30 minutes at room temperature. DNA was then recovered from the isopropanol layer, washed several times with 70% ethanol, and characterized using UV-Vis spectroscopy. Figure 4 shows the UV-Vis spectrum of the isolated DNA.

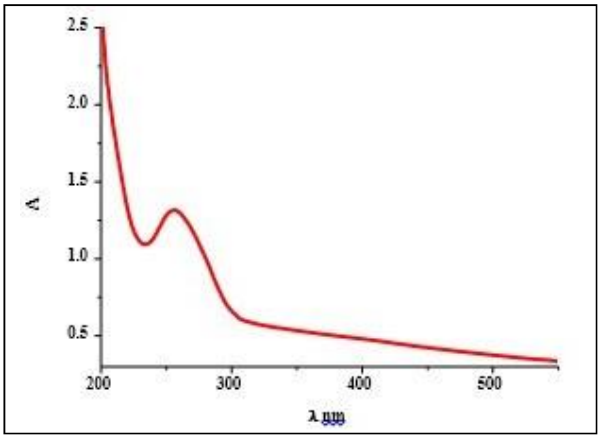

Figure 4. Electronic Spectrum of Extracted DNA Sample

UV-Vis spectroscopy can be used to detect protein contamination in extracted DNA **(Saab et al., 2007).** Proteins exhibit two absorption peaks in the UV region: the first peak is located between 190-210 nm, attributed to electronic transitions in the peptide backbone, and the second peak is situated at 280 nm due to absorption by the aromatic amino acids tyrosine, tryptophan, and phenylalanine **(Khennoufa et al., 2021).**

4.4.1.1. Estimation of DNA Purity:

The isolated DNA cannot be used without further purification as it contains contaminating RNA and proteins. Therefore, the DNA is rehydrated in distilled water, and this dissolution requires continuous agitation overnight at 42°C. The concentration and purity of the DNA can be determined by measuring ultraviolet light absorption. DNA has maximum and minimum absorption at 260 nm and 234 nm, respectively **(Telfer et al., 2013).** The purines and pyrimidines in the nucleic acid are responsible for these absorptions. At 260 nm, double-stranded DNA has a specific absorption coefficient of 0.02 $(\mu g/ml)^{-1}cm^{-1}$ **(Griffiths & Chacon-Cortes, 2014).** Additional-

ly, the ratio of A_{260}/A_{280} can detect nucleic acid purity relative to protein contamination, as proteins have maximum absorption at 280 nm. Highly purified DNA samples have a 260/280 nm ratio of (1.7-1.9), so below (1.7), a significant amount of protein impurities may be present in the sample **(Whitlock et al., 2008).** The A_{260}/A_{230} ratio is determined to confirm that the sample is free from carbohydrates, peptides, ethanol, or any other organic compounds, and it is generally greater than 1.5 **(Ning et al., 2009).**

Therefore, good quality DNA should have:

$$\frac{A_{260}}{A_{280}} = 1.7 \square 2 \qquad \text{and} \qquad \frac{A_{260}}{A_{230}} > 1.5$$

In our study, we used UV-Vis spectroscopy to estimate the purity of the isolated DNA. The absorbance values of the DNA solution obtained were measured at 230, 260, and 280 nm to determine the concentration and purity of the extracted DNA. The dissolved DNA can be stored at 4°C for a few days or at -20°C for longer-term storage (Heckel et al., 2017). The absorbance values were taken from Figure 3 and listed in Table 2. The values obtained for the various absorbance ratios indicate the high purity of the isolated DNA.

Table2. Absorbance Ratio of Isolated DNA

A230	A260	A280	A260/A230	A260/A280
1.116	1.301	1.021	1.166	1.724

✓ Estimation of DNA Quantity:

The quantity of DNA was determined by absorption spectroscopy using the molar extinction coefficient value of 6600 $M^{-1}cm^{-1}$ at 260 nm (Schöppler et al., 2011).

4.4.2. Cyclic Voltammetric Measurements:

✓ Apparatus:

The apparatus used for voltammetric measurements is a Potentiostat/Galvanostat Model PGZ301 (Radiometer Analytical SAS) connected to a three-electrode electrochemical cell,

- A glassy carbon electrode with a diameter of 5.2 mm^2.
- A mercury/mercurous chloride/saturated KCl reference electrode.
- A platinum auxiliary electrode with a diameter of 3 mm^2.

All of this is controlled by a Pentium IV microcomputer (CPU 4.0 GHz and RAM 2 GB) equipped with VoltaMaster4 software, version 7.08.

✓ Reagents:

- Potassium phosphate buffer solution
- Electrolyte support (Tetra-n-butylammonium tetrafluoroborate, 99%)
- Ethanol
- Nitrogen (Gas)
- Ultra-pure water

✓ Procedure:

The reaction between the essential oils and the DNA/BSA takes place in the electrochemical cell. The reaction medium is a buffer solution consisting of a mixture of monopotassium and dipotassium phosphate (KH_2PO_4+K_2HPO_4) at 0.1 M and pH 7.2.

Before each measurement, the working electrode is polished using p4000 abrasive paper. After polishing, the electrode is washed with ultra-pure water and dried with air. The surface of the electrode thus appears mirror-like. Then, the electrochemical cell is equipped with the reference electrode and the auxiliary electrode, as well as the working electrode. The cell is filled with 10 ml of a solution consisting of 90% ethanol/buffer solution containing the essential oils under study. Nitrogen gas is bubbled through the solution for 10 to 15 minutes to remove oxygen from the cell. A variable potential is applied at a fixed scan rate and at a temperature of 28 ± 2°C. The obtained voltammogram is analysed to access the interaction parameters between the studied essential oil and the DNA/BSA.

4.4.3. Spectroscopic Measurements:

✓ Apparatus:

UV-Vis measurements were performed using a UV-Vis spectrometer (Shimadzu 1800) and a quartz cell with a volumetric capacity of 5 ml. Data acquisition was carried out with a Pentium IV microcomputer (CPU 4.0 GHz and RAM 2 GB) equipped with UV probe software version

2.34 (Shimadzu). The data is processed using OriginLab 9.0 software.

✓ Reagents:

- Potassium phosphate buffer solution
- Ethanol
- Ultra-pure water

✓ Procedure:

The electronic spectra of essential oil in the 90% ethanol/potassium phosphate buffer solution were obtained in the absence and presence of increasing concentrations of DNA/BSA.

4.5. In-Silico Evaluation of the Biological Activities

4.5.1. ADMET and drug-likeness evaluation

Drug candidates should possess favourable ADMET properties and ideally non-toxic. Therefore, the major identified compounds from the essential oils extract were evaluated of their ADME profile, including physicochemical, lipophilicity, water solubility, pharmacokinetics, drug-like nature, medicinal chemistry, and several other parameters using SwissADME **(Daina et al., 2017; Riyadi et al., 2021)** module provided in SIB (Swiss Institute of Bioinformatics) webserver **(https://www.sib.swiss).** Furthermore, the toxicity aspect of designed compound was also predicted using ProTox **(Banerjee et al., 2018) (https://comptox.charite.de/protox3/)**.

4.5.2. Docking setup:

- Ligands preparation:

The three-dimensional configurations of the major compounds isolated from *Origanum Majorana L* essential oil were obtained from the National Library of Medicine (NCBI) database **(Kim et al., 2016)**, accessible through the NCBI website **(https://pubchem.ncbi.nlm.nih.gov/).**

Ligand preparation involved an energy optimization process to derive the most energetically favourable conformations for each compound. Utilizing LigPrep module within the Schrödinger suite **(Schrödinger, 2024)**, this optimization procedure ensured the attainment of the lowest energy state for the studied drugs, including Montbretin A (a co-crystallized ligand). The ionization states were established at a pH of 7.0 ± 2.00, as computed by the Epik classic module, while maintaining specified chirality and generating relevant tautomeric forms. Furthermore, partial atomic charges were computed using Optimized Potentials for Liquid Simulations OPLS4 force field **(Lu et al., 2021)**.

- Receptor Preparation:

The 3D structures of receptors, including the human DNA receptor (PDB ID: 1W0T) **(Court et al., 2005)**, bovine serum albumin (PDB ID: 6QS9**) (Castagna et al., 2019),** Escherichia coli (PDB ID: 6F86) **(Narramore et al., 2019),** Bacillus subtilis (PDB ID: 2VAM) **(Oliva et al., 2007)** and Klebsiella pneumoniae (PDB ID: 3QVJ) **(French et al., 2011).** Information regarding the receptors, including their names and PDB IDs, has been listed in the following Table 3.

Processing of the protein structures was executed through the "protein preparation Work-

flow" module within the Schrödinger suite **(Madhavi Sastry et al., 2013)**, involving consecutive stages of import and processing, review and modification, and refinement.

In the initial stage, the Prime tool was employed to address missing residues and side chains, maintaining the pH of PROPKA at 7.0 ± 2.00. Subsequent steps included the optimization and assignment of hydrogen bonds, along with the removal of water molecules beyond 8 Å. Restrain minimization utilizing the Optimized Potentials for Liquid Simulations (OPLS4) force field was performed to achieve a low-energy state for the protein **(Lu et al., 2021).** This phase of protein preparation signifies an energy optimization methodology, presenting the protein in its energetically favourable state for subsequent *in-silico* studies.

The "Receptor grid generation" panel facilitated the creation of a grid encompassing the active site of the protein, delimited by the co-crystallized ligands. Default parameters were maintained, and the grid centre was generated in the active site of the targeted proteins.

Table3. The information related to the selected target receptors for molecular docking studies

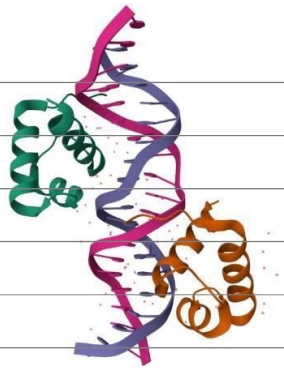	hTRF1 DNA-binding domain in complex with telomeric DNA	
	PDB ID	1W0T
	Mutation	No
	Resolution (Å)	2.00
	R-Value Observed	0.252
	Organism	Homo sapiens
	Space Groupe	P 21 21 21
	Sequence Length	53
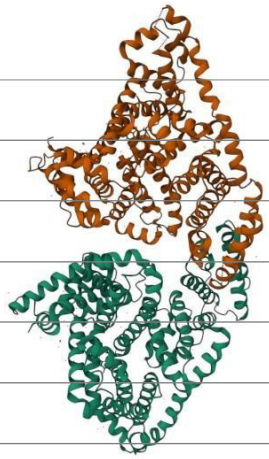	Bovine Serum Albumin in complex with Ketoprofen	
	PDB ID	6QS9
	Mutation	No
	Resolution (Å)	2.80
	R-Value Observed	0.218
	Organism	Bos taurus
	Space Groupe	C 1 2 1
	Sequence Length	607

➢ Molecular Docking:

Computational simulations, including Induced Fit Docking, molecular dynamics studies, and MM-GBSA calculations, were conducted employing the Glide module, Induced Fit Docking module, Prime module, and the Desmond module within the Maestro version 11.7 user interface of the Schrödinger suite **(Small-Molecule Drug 2021) (Schrödinger, 2015)**. The simulations were executed on a DELL Intel(R) Core(TM) i9-13900HX CPU @ 2.20 GHz processor, equipped with 32,0 GB RAM, and operated on a 64-bit Linux Ubuntu 18,04.1 LTS operating system.

The molecular docking tool employed for all docking studies was Glide (Grid-based Ligand docking with Energetics), a module within the Schrödinger suite **(Yang et al., 2021)**. The prepared ligands underwent docking onto the specified protein site utilizing the Glide module, in Standard Precision (SP) modes **(Friesner et al., 2006**).

➢ Induced Fit Docking (IFD):

The Induced Fit docking (IFD) module of the Maestro molecular modelling suite has been noted as a reliable and effective docking approach to consider flexibility in both ligands and the binding pocket residues in the binding pocket of target receptors **(Khelil et al., 2020).** During the IFD process, Glide/SP (Standard Precision) was performed for each ligand, the Prime refinement step specifically addressed the side chains of residues within a 5 Å radius of the ligand. Noteworthy is the retention of a maximum of 20 poses for each ligand.

➢ Molecular Dynamics Simulation (MDS):

The best compound in exhibiting the highest IFD docking score was chosen for Molecular Dynamics Simulation (MDS). Recognizing the limitations of ligand docking in representing the biological system under aqueous conditions **(Korb et al., 2012)**, a 100 ns simulation time for MDS was executed using the Desmond module within the Schrödinger suite **(Bowers et al., 2006)**.

The MDS protocol comprised three essential steps: system builder, minimization, and MDS. In the system builder phase, the protein and ligand complex were selected and immersed in a biological environment. The transferable intermolecular potential with 3 points (TIP3P) solvent model, with the boundary condition maintained in an orthorhombic box form throughout the process with dimensions of 10 x 10 x 10 Å **(Akbar et al., 2022).** The OPLS-3e force field was consistently applied **(Roos et al., 2019).** The neutralization of model was conducted by addition of counter ions when needed and 0.15 M of NaCl salt was included to mimic the physiological state.

Subsequently, the NPT ensemble was utilized for energy minimization, maintaining pressure and temperature at 1.0132 bar and 300 K, respectively. Finally, MDS was conducted for the minimized protein-ligand complex **(Halder et al., 2023).**

➢ Free Energy (MM-GBSA) Calculation:

Upon completion of the dynamic simulation, an assessment of the free binding energy between the protein and the ligand was systematically undertaken utilizing the Prime MM- GBSA module within the Maestro molecular modelling suite **(E. Wang et al., 2021).** The calculation of ligand binding affinities was accomplished through the Molecular Mechanics/Generalized Born Surface Area ΔG (MM-GBSA ΔG) metric applied to the optimized Receptor-Ligand Complex. This computation, facilitated by the VSGB solvation model and the OPLS4 force field, stands as a methodologically rigorous approach for the comprehensive evaluation of molecular interactions and binding strengths **(Gorla et al., 2021).**

CHAPTER 2:

Results and discussion

1. Introduction:

This chapter delves into the findings regarding the extraction yield, characterization, and comprehensive exploration of the anticancer and antibacterial properties inherent in the essential oil derived from the aerial constituents of *Origanum Majorana L*. The overarching aim of this investigation was to assess the potential anticancer and antibacterial efficacy exhibited by essential oil as significant agents in the domain of novel pharmaceutical development.

The elucidations provided herein furnish intricate insights into the chemical constitution of the essential oils, thereby enabling their utilization in the *in-silico* study. This involved the application of advanced computational techniques such as Induced Fit Docking (IFD) for each compound, capabilities not feasible in traditional *in vitro* studies.

2. Extraction Yield:

Figure 5 illustrates the yields of essential oils obtained through hydrodistillation of the aerial parts of *Origanum Majorana L*. variety of Eloued.

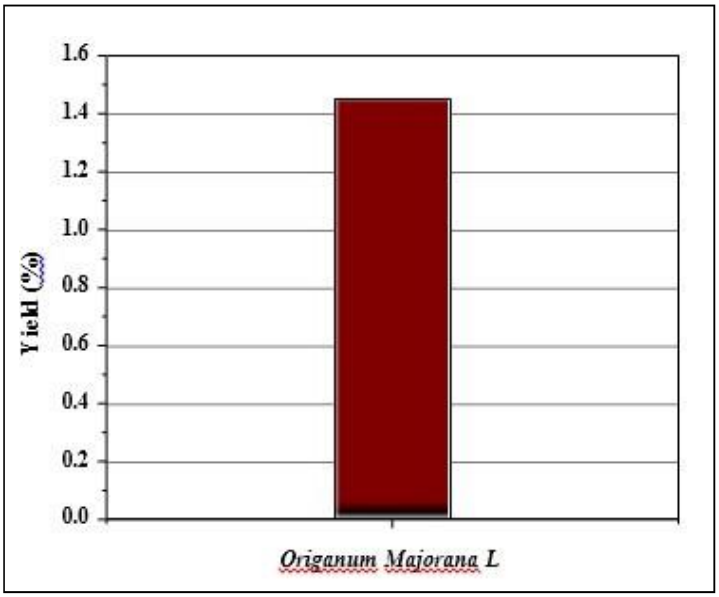

Figure 5. The yields of extracted essential oil

We observe that *Origanum Majorana L* exhibits a good essential oil yield (1.45%).

Nevertheless, findings reported by **(Alimi et al., 2022)** indicate lower yields of essential oils extracted by hydrodistillation from *Origanum Majorana L* at ambient temperature.

Similar results to ours were, however, obtained by **(Naima et al., 2019)** for the essential oil extracted from the same variety using the same method.

Furthermore, significantly higher yields were achieved by **(Vera & Chane-Ming, 1999)** during the hydrodistillation of *Origanum Majorana L*, Indian variety.

These variations in results can be explained by the fact that essential oil yields are influenced by several factors during extraction: either factors related to the plant (species, variety, chemical composition, etc.) or factors associated with experimental conditions (extraction process, extraction duration, etc).

3. Chemical composition of essential oils

3.1. Organoleptic characteristics:

Through the conducted work, it has been revealed that the essential oil extracted from the studied plant exhibits the following (Table 4) organoleptic properties:

Table4. The organoleptic characteristics of essential oils

Plant	Smell	Aspect	Colour
Origanum Majorana L	A pleasant fragrance	liquid at room temperature	Light-yellow

3.2. Physicochemical Properties:

The physicochemical properties were meticulously determined according to the standards of the French Association for Standardization (AFNOR) using established methodologies to measure relative density, refractive index, acidity index, and ester index, as depicted in the following Table 5.

Table5. The physicochemical properties of essential oils

Plant	Relative Density	Refractive Index	Acidity Index	Ester Index
Origanum Majorana L	0.908	1.4512	4.39	41.23

By comparing these results to those obtained by **(Naima et al., 2019)** (density 0.953, refractive index 1.474, acidity index 4.93 and ester index 45.96) and **(Alimi et al., 2022)** (density: 0.834 ± 0.02, refractive index, at 25°C 1.4596 ± 0.03), and considering that the refractive index was measured at a temperature of 23°C, we can conclude that these values are in accordance with the standards described by AFNOR **(Afnor, 1982).**

3.3. Gas Chromatography-Mass Spectrometry (GC/MS) analysis:

The analysis focused on the essential oil constituents extracted from specific plant species using gas chromatography-mass spectrometry (GC/MS). Mass spectra corresponding to each chromatographic peak were juxtaposed with spectra from relevant scientific literature and the Weily electronic database for mass spectra **(Horai et al., 2010)**. Retention indices were employed to ascertain compound identities. Moreover, utilizing the identical non-polar HP5 stationary phase in the gas chromatography column facilitated the preservation of consistent peak numbers and elution sequences for the compounds under investigation.

Figure 6 depict the chromatograms illustrating the essential oil compositions of *Origanum Majorana L*, as obtained through gas chromatography-mass spectrometry (GC/MS) analysis:

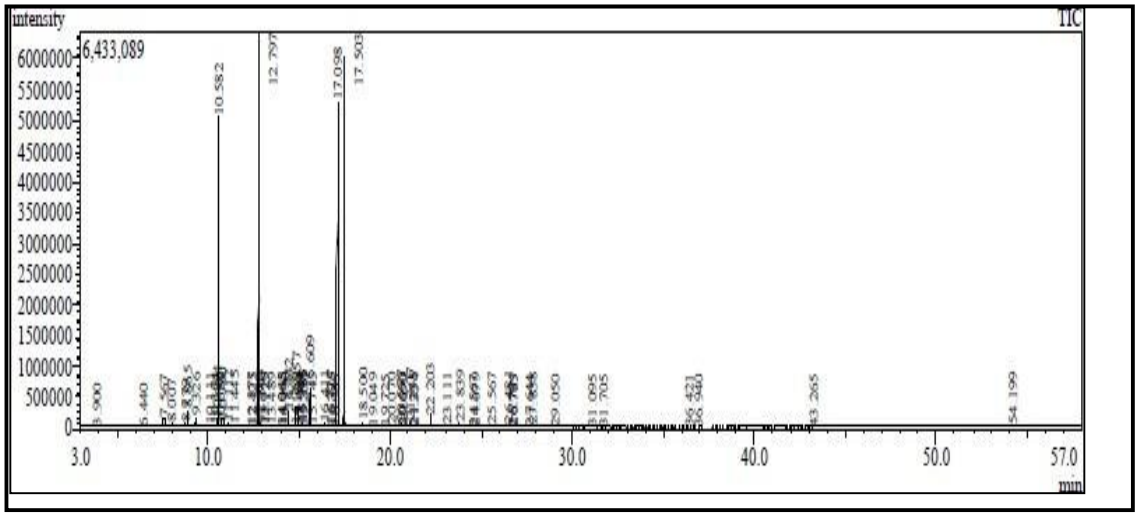

Figure6. Chromatogram of the essential oil of *Origanum Majorana L* plant obtained by GC/MS

Upon scrutinizing the obtained chromatogram, notable resemblances are evident, with discernible bands interspersed with overlapping ones. Generally, distinct regions can be identified, delineating three segments:

1. The initial segment, delimited within the time frame of (4 min to 12.4 min), hosts several bands denoting the presence of hydrocarbon monoterpenes.
2. The succeeding segment, spanning from (12.4 min to 24 min), encompasses the predominant bands, indicative of oxygenated monoterpenes prevalent in the plant's essential oil.
3. The final segment, spanning (24 min to 32.5 min), exhibits minimal banding, suggesting a negligible presence of hydrocarbon sesquiterpenes in the plant's e sential oil.

The pertinent compounds in each essential oil, extracted from *Origanum majorana L*, have been identified and collated as follows

3.3.1. Origanum Majorana L

The hydrodistillation extraction method was employed to obtain the essential oil from *Origanum Majorana L*., yielding a noteworthy 1.45% output. Analysis revealed the identification of 98.84% of the constituents, comprising a total of 42 compounds (as presented in Table 6). Oxygenated monoterpenes dominated the composition, constituting over 57%, followed by hydrocarbon monoterpenes at 25.14%.

Of particular interest is the prominent presence of trans-Thujone, constituting 33.3% of the essential oil, a compound conspicuously absents in the majority of prior studies. For instance,

J. Chane et al.'s **(Vera & Chane-Ming, 1999)** investigation reported Terpinen-4-ol as the primary compound at 38.4%, a constituent entirely absents in our study. Similarly, Santolina triene emerged as the second major compound in our analysis at 16.40%, a finding not corroborated in extant literature.

Despite these disparities, concordance exists with previous studies regarding the occurrence of Sabinene, which manifested at 3.12% in our study, compared to 15% in J. Chane et al.'s **(Vera & Chane-Ming, 1999)** study and 17% in K.H.C Baser et al.'s study **(Baser et al., 1993)**. Additionally, Sellami et al **(Sellami et al., 2009)** documented Sabinene at 2.14%. Supplementary compounds identified include α-Thujene (1.44%), α-Pinene (1.19%), and β- Pinene oxide (4.42%).

In summary, the essential oil derived from *Origanum Majorana L*. exhibits distinctive chemical compositions in Eloued region compared to oils from other geographical locales, characterized notably by the prevalence of trans-Thujone and Santolina triene as major constituents. This variance likely stems from multifactorial influences such as soil quality, climatic conditions, and harvest timing. For an illustrative overview of the major compounds identified, Figure 7, displaying the structures and IUPAC nomenclature of these constituents.

Table6. Essential oil constituents of Origanum Majorana L identified by GC/MS

No	Compounds	IR_{Exp}	IR_{Ref}	(%)
01	Pentanol	759	762	0.12
02	Cis-2-Penten-1-ol	762	765	0.03
03	Hexanal	801	801	0.02
04	(Z)-Salvene	844	847	0.02
05	Isopentyl acetate	869	869	0.02

06	**Santolina triene**	**898**	**906**	**16.42**
07	Tricyclene	912	921	0.02
08	**Alpha-Thujene**	**918**	**924**	**1.44**
09	**Alpha-Pinene**	**925**	**932**	**1.19**
10	Camphene	941	946	0.43
11	**Sabinene**	**969**	**969**	**3.12**
12	Beta-Pinene	972	974	0.22
13	Beta-Myrcene	989	988	0.14
14	Alpha-Phellandrene	1003	1002	0.03
15	ropanoic acid, 2-methyl-, 3-methylbutyl ester	1012	1007	0.02
16	Alpha-Terpinene	1016	1014	0.36
17	Para cymene	1024	1020	0.20
18	Ortho Cymene	1026	1022	0.45
19	Sylvestrene	1028	1025	0.20
20	**1,8-Cineole**	**1031**	**1026**	**10.71**
21	Trans-decahydroNaphthalene	1054	1053	0.03
22	Terpinene	1059	1054	0.76
23	Cis Sabinene hydrate	1068	1065	0.89
24	Para-Mentha-2'4(8)-diene	1088	1085	0.11
25	Trans-Sabinene hydrate	1100	1198	0.86
26	Isopentyl-2-methylbutanoate	1104	1100	0.14
27	cis-Thujone	1107	1101	0.24
28	**trans-Thujone**	**1119**	**1112**	**33.30**
29	iso-3-Thujanol	1136	1134	0.04
30	**Camphor**	**1146**	**1141**	**2.85**
31	**Beta pinene oxide**	**1163**	**1154**	**4.42**
32	3-Thujanol	1168	1164	0.48
33	Alpha Terpineol	1192	1186	0.88
34	Dihydrocarveol	1197	1192	0.06
35	Safranal	1203	1197	0.01
36	Cis-3-Hexenyl 2-methyl buta-noate	1233	1229	0.25
37	trans-Myrtanol	1257	1258	0.04

38	2-(1E)-propenyl Phenol	1258	1264	0.09
39	**cis Verbenyl acetate**	**1277**	**1280**	**15.05**
40	neoiso-3Thujanol acetate	1287	1281	0.09
41	Isobornyl acetate	1290	1283	0.21
42	Lavandulyl acetate	1293	1288	0.32
	Total		**95.64**	

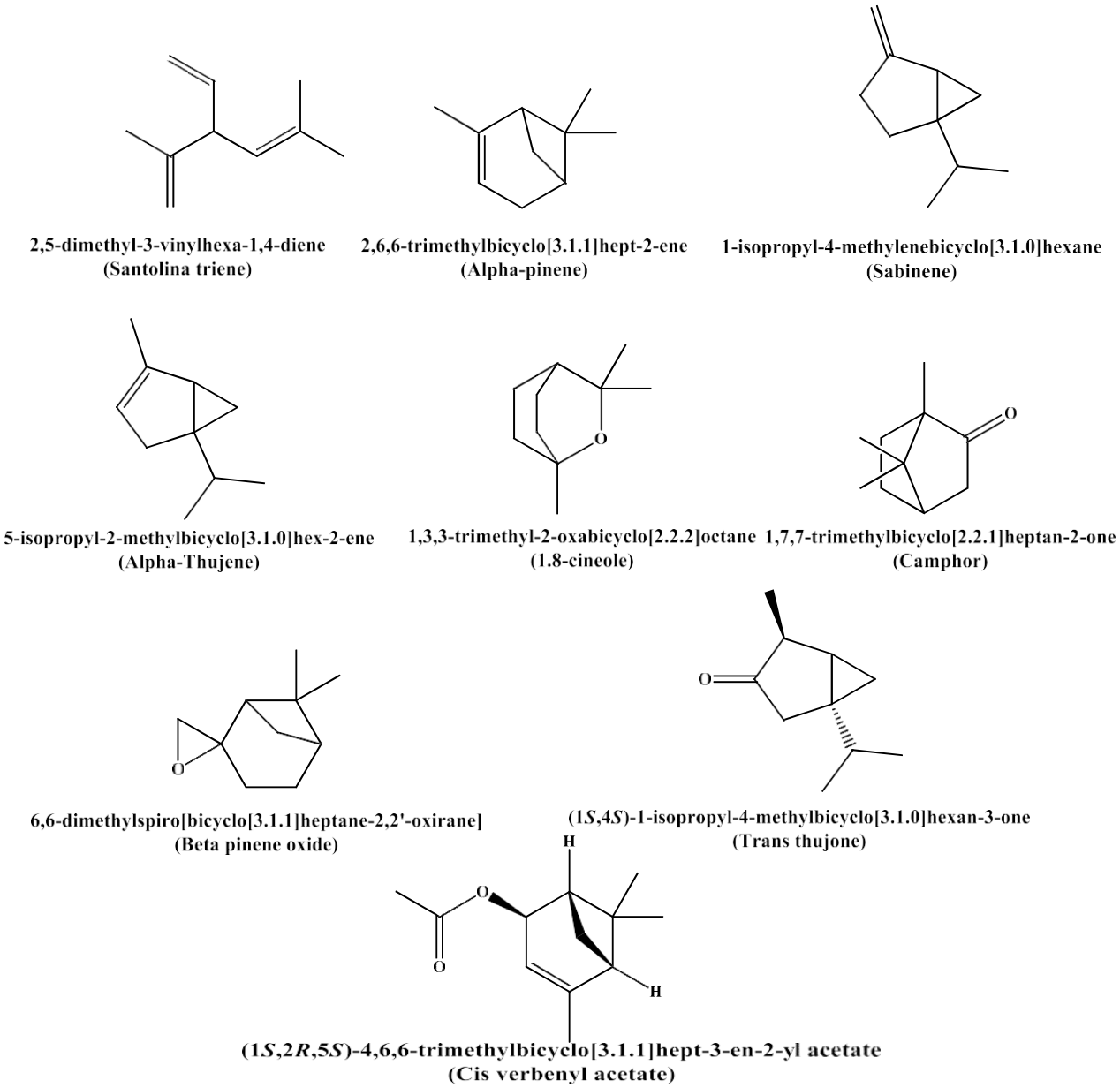

Figure 7. Chemical structures and IUPAC names of the top major compounds identified in the essential oil of *Origanum Majorana L*

4. DNA Interaction Study

4.1. Electrochemical DNA interaction study

4.1.1. Binding constants:

When an increasing concentration of DNA was added to a solution of essential oil, the anodic peak current height of this essential oil was decreased. Also, during DNA addition, anodic peak potential showed a displacement in the negative going direction, Figure 8. These results indicated that the studied essential oil interact with DNA by electrostatic mode **(E. Lanez et al., 2019; Mouada et al., 2019)**, Figure 8 further indicates that in the absence of DNA, the voltammograms of *Origanum Majorana L* essential oil show an anodic peak potential at 1.201 V. While in the presence of 0.81, 1.62, 2.41, 3.18, 3.94, 4.68, 5.41, 6.13, 6.83 and 7.52 µM

DNA, these peaks appear at 1.2, 1.201, 1.202, 1.203, 1.204, 1.205, 1.206, 1.207, 1.208 and

1.209 V respectively, with an apparently negative shift of 1 mV by each increasing of concentration indicating that there exists interaction between the studied essential oil and DNA. The voltammograms also show a drop in the anodic peak current densities. This drop can be attributed to slow diffusion of the formed DNA-EO adducts.

The peak potential shift in the cyclic voltammetric behavior of the essential oil by the addition of DNA is attributable to the electrostatic interactions between the compounds and DNA, an indicator of the oxidizable behavior of the compounds in the presence of negative environment of DNA.

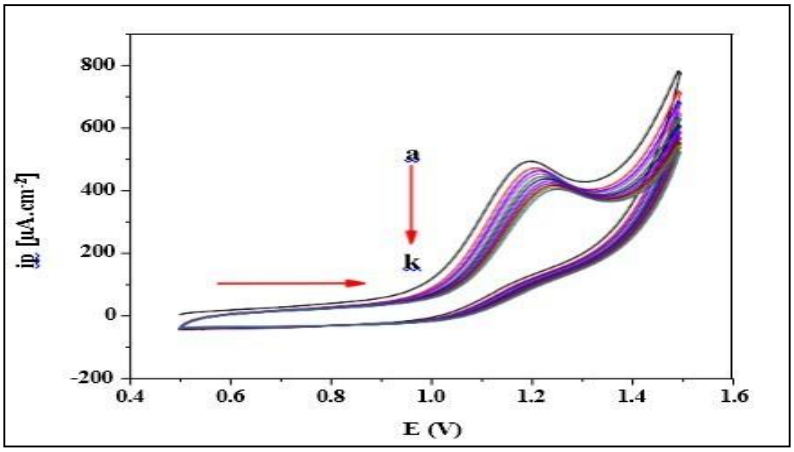

Figure 8. Cyclic voltammograms of 2 mM *Origanum Majorana L* essential oil recorded at 0.1V s^{-1} potential sweep rate on GC disk electrode at 298K in the absence and presence of increasing concentration of DNA in 0.1 M 90% ethanol/buffer phosphate solution at pH =7.2 with supporting electrolyte 0.1 M Bu_4NBF_4

Generally, the negative shift in formal potential caused by the addition of a potentially drug to DNA is caused by the electrostatic interaction of the cationic drug DNA backbone **(Jamil et al., 2013; Shah et al., 2010)**, so the obvious negative peak potential shift (anodic shift) in the CV behaviour of essential oil by the addition of DNA can be attributed to the electrostatic interaction (H-bonding) between EO and the DNA. This negative peak potential shift further indicates that the compounds in the essential oil left over is easier to oxidize in the presence of negative environment of DNA. Further addition of DNA diminishes the oxidation peak which supports the participation the compounds present in the essential oil in hydrogen binding with DNA, and not let electrons to go out of the system (Figure 8).

The decrease in anodic peak current density of EO-DNA adduct relative to free EO is used for the calculation of the binding constants and binding free energies using Equation 6 **(Zhao et al., 1999)**:

$$\text{Log}\ \frac{1}{[DNA]} = \frac{\log K_b + \log ip}{ip_0 - ip} \quad \ldots\ldots\ldots \textbf{(6)}$$

where $[DNA]$ is the DNA concentration (M); K_b represents the binding constant (M^{-1}); ip_0 and ip denote the anodic peak current density of the free and DNA-bound compound, respectively ($\mu A/cm^2$).

The plot of log $1/[DNA]$ versus log $1/1-(i/i_0)$ gave a straight line (Figure 9) with a 'y' intercept equal to the logarithm of binding constant K_b.

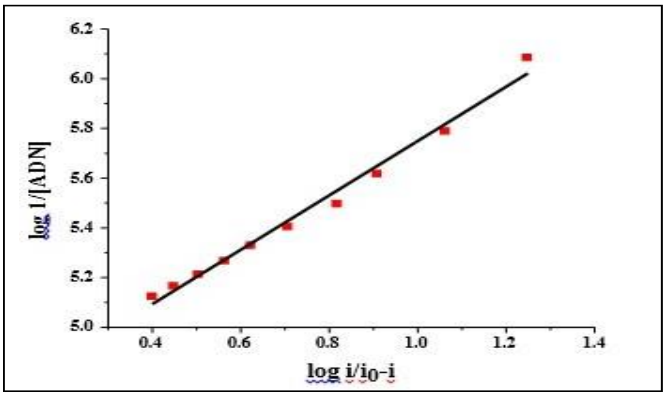

Figure9. Plots of $\boldsymbol{log\ (1/1-(i_p/i_{p_0}))}$ versus $\boldsymbol{log\ 1/[DNA]}$ used to calculate the binding constants of studied essential oil with DNA

4.1.2. Binding free energy:

The binding free energy change was calculated using the following Equation 7

$$\Delta G = \Delta RT \ln K_b \quad \text{(7)}$$

where ΔG is the binding free energy in KJ.mol^{-1}, R is the gas constant, 8.32 J.mol^{-1}K^{-1} and T is the absolute temperature, 298K.

Binding parameters of the studied essential oil are listed in Table 7

Table7. Binding constant and binding free energy values for EO with DNA from CV data

Adduct	Equation	R^2	K (M^{-1})	-ΔG (KJ.mol^{-1})
EO_DNA	y = 1.092x + 4.651	0.985	4.48×10^4	26.55

4.1.3. Diffusion coefficients

Figure 10 shows the electrochemical behavior of the EO at different scan rates. The volt-ammograms displayed clear stable anodic peaks. The diffusion coefficients of the free and DNA bound form was determined using the Randles-Sevcik Equation 8 **(Husain et al., 2015)**:

$$ip_a = 2.69\times10^5 \left(\sqrt{n}\right)^3 SC \sqrt{D}\sqrt{v} \quad \text{…….. (8)}$$

where ip_a is the peak current density (A), n is the number of electrons transferred during the oxidation, S is the surface area of the electrode (cm^2), C is the bulk concentration (mol.cm^{-3}) of the electro-active species, D is the diffusion coefficient (cm^2.s^{-1}), and v is the scan rate (V.s^{-1}).

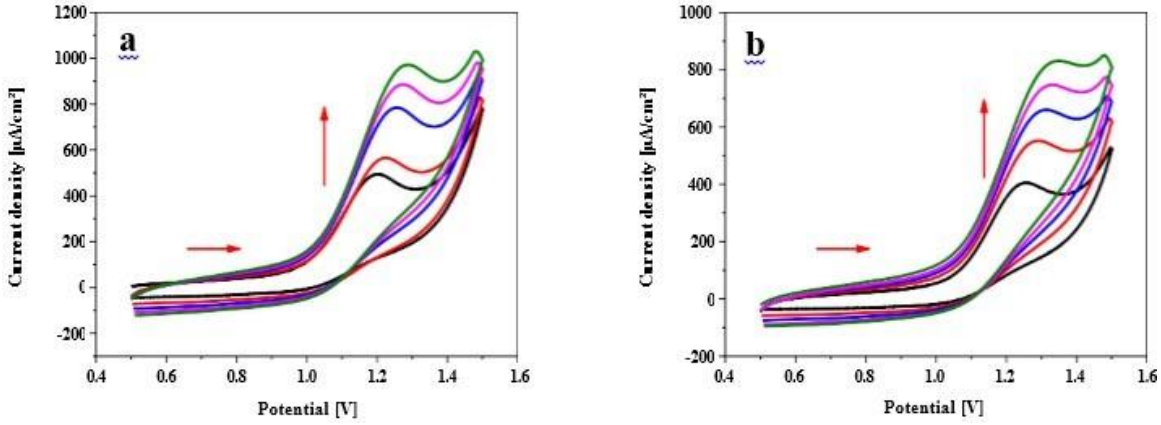

Figure 10. Cyclic voltammetric behavior of *Origanum Majorana L* essential oil on GC electrode in the absence (a) and in the presence of respectively, 7.52 µM DNA in 0.1 M 90% ethanol/buffer phosphate solution at pH = 7.2 and scans rates 0.5, 0.4, 0.3, 0.2 and 0.1 $V.s^{-1}$ with supporting electrolyte 0.1 M TBATFB. The vertical arrowhead indicates increasing scan rate

The plots of the square root of the scan rates versus the anodic peak current density, (Figure 11), suggest that the redox process is diffusion controlled. The value of the diffusion coefficient is $D = 5.027\times10^{-6}$ $cm^2.s^{-1}$ was deducted from the slope of the linear regression of Equation 9. Furthermore, the formal potential values are almost infected by the increasing of scan rate values.

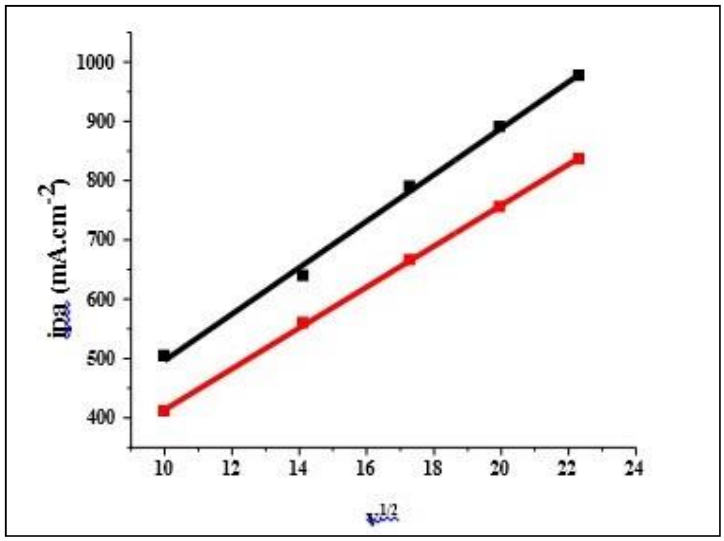

Figure 11. Plots of $\sqrt{v}$ versus i_p used to calculate the coefficients diffusion of free (Black line) and bounded DNA (Red line)

Table8. Diffusion constants values of the free and DNA bound forms

Compound	Equation	R^2	$D(cm^2.s^{-1})$
EO	y = 39.203x + 104.06	0.995	5.027×10^{-6}
EO_DNA	y = 34.307x + 71.436	0.999	3.85×10^{6}

The diffusion coefficient provides crucial insights into the nature of molecular interactions, particularly when considering the formation of complexes between molecules **(El-Hallag, 2010)**. When a complex forms between two or more molecules, such as an essential oil and DNA, the resulting complex typically has a higher molecular weight than the individual molecules in their free form. As a result, the diffusion coefficient serves as a measure of the mobility of molecules in a solution **(T. Lanez & Hemmami, 2016).** In the context of a formed complex, the diffusion coefficient tends to decrease compared to the diffusion coefficient of the individual molecules in their free form. This decrease in diffusion coefficient indicates that the formed complex moves more slowly through the solution due to its increased molecular weight **(T. Lanez et al., 2015).**

4.2. Electronic spectroscopy DNA interaction study

Electronic absorption spectroscopy is an effective method for examining the binding mode. The hypochromic effect induced by the DNA on a spectrum of a bound ligand is one indicator of the binding mode. In general, intercalators have stronger hyperchromicities than the corresponding groove binders. The absorption spectra of essential oils bound to DNA through intercalation exhibit significant hypochromic and red shift due to the strong $\pi\rightarrow\pi^*$ stacking interaction between the aromatic chromophore ligand of metal complex and the base pairs of DNA **(Shah et al., 2010).**

To get complementary method to the voltammetry techniques, electronic spectroscopy titration was performed to study the interaction of essential oil with DNA in buffer phosphate solution (KH_2PO_4/K_2HPO_4) at pH = 7.2. The absorption spectra of a fixed concentration (2 mM) of *Origanum Majorana L* essential oil in the absence and presence of gradually increasing concentration of DNA stock solution are shown in Figure 12. In the visible region, *Origanum Majorana L* essential oil has one absorption peaks at 239 nm, (Figure 12). Upon addition of DNA, a significant hyperchromicity was observed without any noticeable shift in the position of maximum absorption peak that clearly indicated the formation of adduct between DNA and the studied essential oil **(Rakesh et al., 2012).** Hyperchromicity further suggesting mainly groove binding property of EO compounds to the double-stranded DNA **(Shahabadi et al., 2011).**

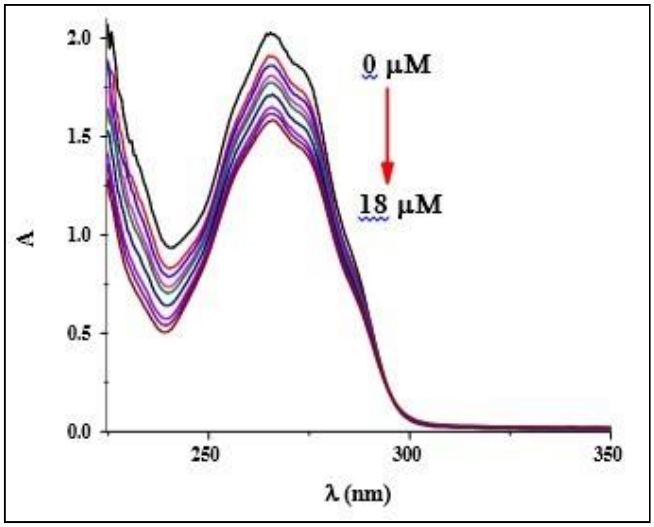

Figure12. UV-visible absorption spectra of 2 mM of *Origanum Majorana L* essential oil in presence of increasing concentrations of DNA in 0.1 M 90% ethanol/buffer phosphate solution (KH_2PO_4/K_2HPO_4) at pH = 7.2 and 298K

4.2.1. Binding constants:

The change in absorbance values by increasing DNA concentration was used to evaluate the intrinsic binding constant employing the following Equation 9, **(Isaac et al., 1999; Ni et al., 1997).**

$$\frac{A_0}{A - A_0} = \frac{\varepsilon_G}{\varepsilon_{H-G} - \varepsilon_G} + \frac{\varepsilon_G}{\varepsilon_{H-G} - \varepsilon_G} \frac{1}{K_b [DNA]} \quad \text{…….. (9)}$$

where $[DNA]$ is the DNA concentration, K_b is the binding constant, $A_0$and A are respectively the absorbance of ligand in the absence and presence of DNA, and ε_G and ε_{H-G} are their extinction coefficient respectively.

The constant K_b is obtained from the intercept to slope ratio of the plot of $A_0/(A - A_0)$ versus$1/[DNA]$, Figure 13..

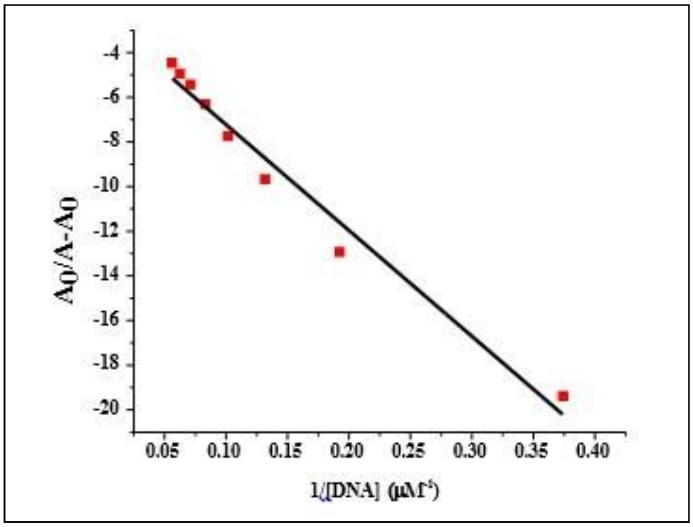

Figure13. Plots of $\boldsymbol{A_0/(A - A_0)}$ versus $\boldsymbol{1/[DNA]}$ used to calculate the binding constants of *Origanum Majorana L* essential oil with DNA

4.2.2. Binding free energy:

The binding free energy change was calculated using the following Equation 10 (W., 1998)

$$\Delta G = -RT \ln K_b \quad \textbf{(10)}$$

where ΔG is the binding free energy in KJ.mol^{-1}, R is the gas constant, 8.32 J.mol^{-1}K^{-1} and T is the absolute temperature, 298K. Binding parameters are listed in Table 9.

Table 9. Binding constant and binding free energy values for *Origanum Majorana L* essential oil with DNA from UV data

Adduct	Equation	R^2	K (M^1)	-Δ(KJ.mol^{-1})
EO_DNA	y = -2.435x – 47.546	0.998	5.12×10^4	26.89

4.3. Molecular Docking Study:

In the current study, the binding interaction of all the major compounds presented in *Origanum Majorana L* essential oils with human DNA was further investigated by carrying out a molecular docking analysis of the binding interaction between human DNA with compounds: trans thujone, alpha-Terpineol, beta-Terpineol, cis Verbenyl acetate, Camphor, Sabinene, gamma terpinene, alpha-Pinene, 1,8-Cineole, Santolina triene, alpha-Thujene and Beta Pinene oxide **(**the major phytochemicals present in the two plants with yield > 1) using Maestro version 11.7 user interface of the Schrödinger suite (Small-Molecule Drug Discovery Suite 2021-4, Schrödinger, LLC, New York, NY, 2021) **(Schrödinger, 2015).**

Each compound was docked with human DNA to understand their interactions at the en-

zyme's active site. Of all the major compounds present in *Origanum Majorana L* essential oils, the binding affinities of them for DNA were comparable to that obtained by CV and UV (Table 10). This result indicates that the plant is a rich source of compounds which, either individually or synergistically, resulted in the decrease of the activity of DNA as observed in the *in vitro* experimental DNA interaction study. Also, the interactions were spontaneous as observed from the negative Gibb's free energy values **(Avwioroko et al., 2020).**

Table 10. Docking score of the studied compounds

Compound	Rigid Docking Score (Kcal/mol)	IFD scores (Kcal/mol)
trans thujone	-5.569	-6.679
cis Verbenyl acetate	-4.944	-6.054
Camphor	-4.505	-5.615
alpha-Thujene	-4.41	-5.522
Sabinene	-4.365	-5.475
Beta Pinene oxide	-4.115	-5.225
alpha-Pinene	-3.884	-4.994
1,8-Cineole	-3.706	-4.816
Santolina triene	-2.986	-4.096

The results in Figure 14 revealed that the best two compounds interacted with the nucleic basis of the active site of the DNA via electrostatic interaction. Furthermore, it also confirmed the possibility of the binding interaction between DNA and the phytoconstituents of *Origanum Majorana L* essential oils investigated and observed using spectroscopic and cyclic voltametry methods reported. The best ligand-binding poses in the DNA obtained after docking are as illustrated in Figure 14.

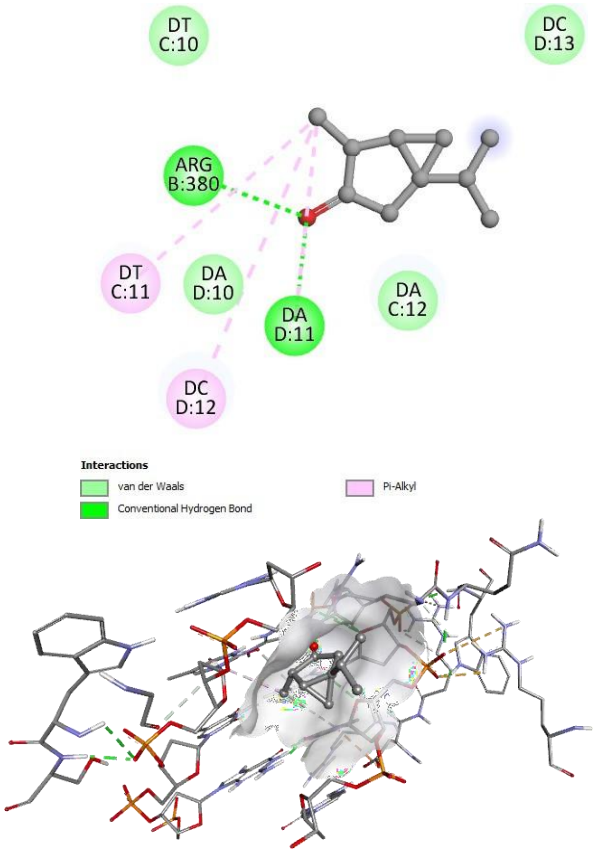

Docking complex and interaction plot for compound trans- thujone with DNA

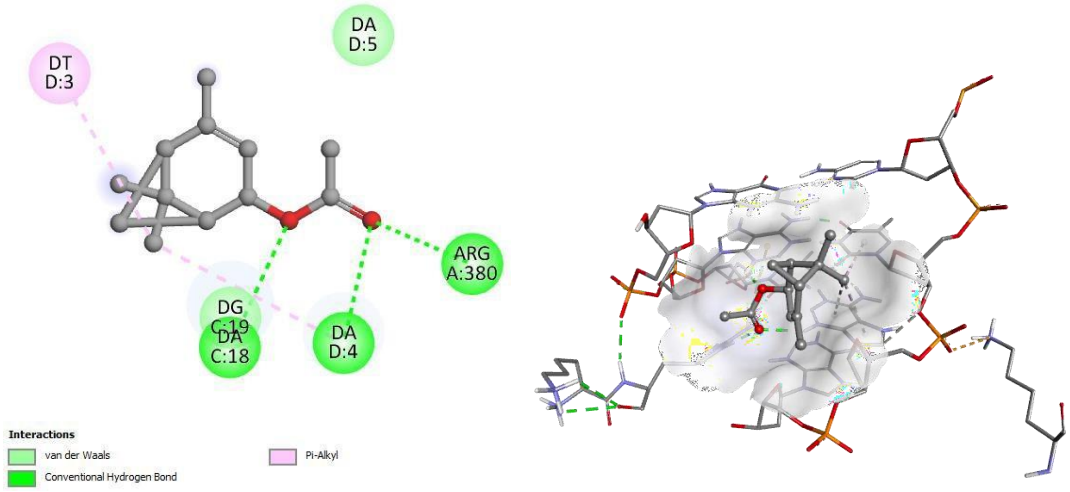

Docking complex and interaction plot for compound cis Verbenyl acetate with DNA

Figure14. Molecular interactions of studied compounds with humane DNA **(Personal work.,2024)**

5. BSA Interaction Study:

5.1. Electrochemical BSA interaction study:

The protein binding studies of the extracted *Origanum Majorana L* essential oil were performed by cyclic voltametry based experiments using bovine serum albumin (BSA) in buffer ethanol/buffer phosphate solution at pH = 7.2. The experiments were carried out in the same manner as described for DNA **(Gharagozlou & Boghaei, 2008; Sathyadevi et al., 2011; Topală et al., 2014)**. The method is based on recording the voltammograms of 2 mM solution of essential oil in 0.1 M 90% ethanol/buffer phosphate solution (KH_2PO_4/K_2HPO_4) at pH = 7.2 with supporting electrolyte 0.1 M tetra-n-butylammoniumtetrafluoroborate (Bu_4NBF_4) in the absence and presence of increasing concentration of BSA. After every electrochemical assay the working electrode was polished and the solution was degassed from oxygen via bubbling nitrogen gas for at least 15 minutes.

5.1.2. Binding constants:

As shown in Figure 15, when an increasing amount of BSA was added to a solution containing the studied essential oil the anodic peak current density decreased. Also, during BSA addition, the anodic peak potential showed a dislocation in the negative going direction for extract. This finding is a proof that the studied essential oil interact with BSA by electrostatic mode **(Ali et al., 2013; Guo et al., 2007; Moriuchi et al., 2000; Savage et al., 2005)**, Figure 14 further indicates that in the absence of BSA, the voltammograms show an anodic peak potential at 1.66 V. While in the presence of 5.66, 1.0, 37.75, 14.2, 9.06 and 7.55 μM BSA, these peaks appear at 1.68, 1.69, 1.70, 1.71, 1.72, 1.73, 1.74, 1.75, 1.76 and 1.77 V respectively, with an apparently negative shift of 0.01 V, this peak potential shift demonstrate that there exists interaction between the studied essential oil and BSA. Furthermore, the voltammograms also show a drop in both the anodic and cathodic peak current densities. This drop can be attributed to slow diffusion of the formed adducts BSA-EO.

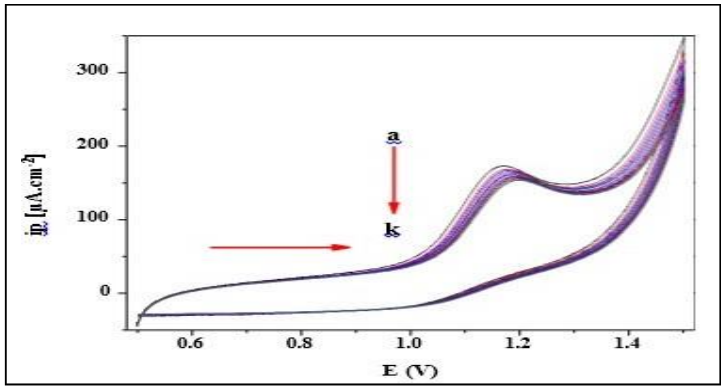

Figure15. Cyclic voltammograms of 2 mM *Origanum Majorana L* essential oil recorded at

0.1V s^{-1} potential sweep rate on GC disk electrode at 298K in the absence and presence of increasing concentration of BSA in 0.1 M 90% ethanol/buffer phosphate solution at pH =7.2 with supporting electrolyte 0.1 M Bu_4NBF_4

The drop in anodic peak current density of EO-BSA adducts relative to the free EO is used for the calculation of the binding constants and binding free energies using Equation 11 **(Zhao et al., 1999):**

$$\log \frac{1}{[BSA]} = \log K_b + \log \frac{ip}{ip_0 - ip} \qquad \text{.....(11)}$$

where [BSA] represents the BSA concentration (M); K_b is the binding constant (M^{-1}); ip_0 and ip denote the anodic peak current density of the free and BSA-bound compound, respectively ($\mu A.cm^2$).

The plot of $\log 1/[BSA]$ versus $\log 1/1-(i/i_0)$ gave a straight line (Figure 16) with a '*y*' intercept equal to the logarithm of binding constant K_b.

5.1.2. Binding free energy:

The binding free energy change was calculated starting from K_b using Equation 10 described previously. Binding parameters of EO-BSA adducts are listed in Table 11.

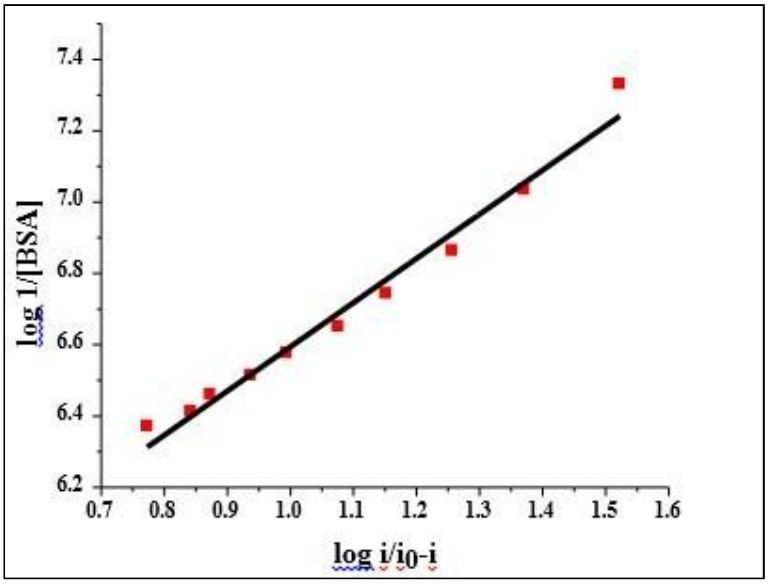

Figure16. Plots of $\boldsymbol{log\ (1/1-(i_p/\ ))}$ versus $\boldsymbol{log\ 1\ /[BSA]}$ used to calculate the binding constants of EO with BSA

Table11. Binding constant and binding free energy values for *Origanum Majorana L* essential oil with BSA from CV data

Adduct	Equation	R^2	K_b (M^{-1})	-ΔG ($KJ.mol^{-1}$)
EO-BSA	y = 1.237x + 5.359	0.976	2.29×10^5	30.60

5.1.3. Diffusion coefficients

Figure 17 shows the electrochemical behavior of the essential oil in different scan rates, in the absence and in presence of BSA. The voltammograms displayed clear stable anodic peaks. The diffusion coefficients of the free and BSA bound form were determined using the Randles-Sevcik Equation.

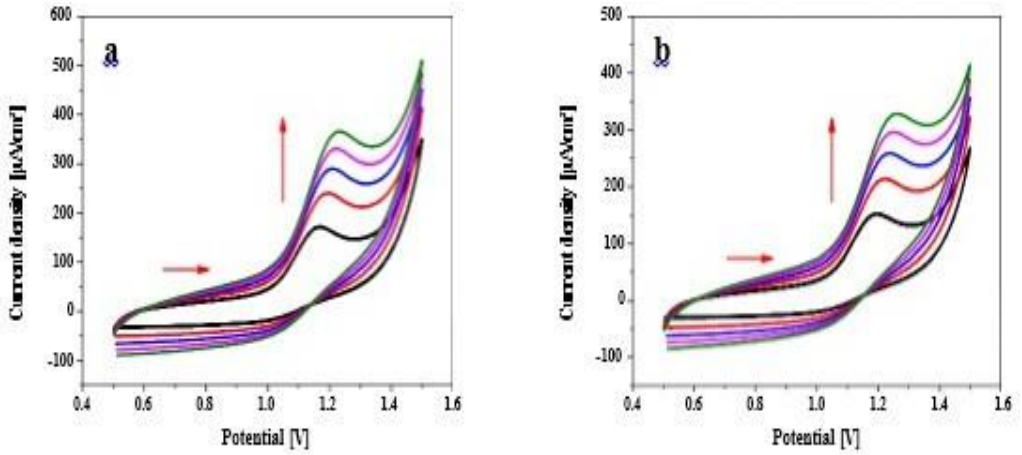

Figure 17. Cyclic voltammetric behavior of *Origanum Majorana L* essential oil on GC electrode in the absence (a) and in the presence of, 0.43 µM BSA in 0.1 M 90% ethanol/buffer phosphate solution at pH = 7.2 and scans rates 0.5, 0.4, 0.3, 0.2 and 0.1 $V.s^{-1}$ with supporting electrolyte 0.1 M Bu_4NBF_4. The vertical arrowhead indicates increasing scan rate

The plots of the square root of the scan rate of potential $\sqrt{V}$ versus the anodic current values i_p for essential oil in the absence and in presence of a given amount of BSA gave a straight line, Figure 18. From the slope of these lines the diffusion coefficients were determined for the free and BSA bound forms, values are summarized in Table 12

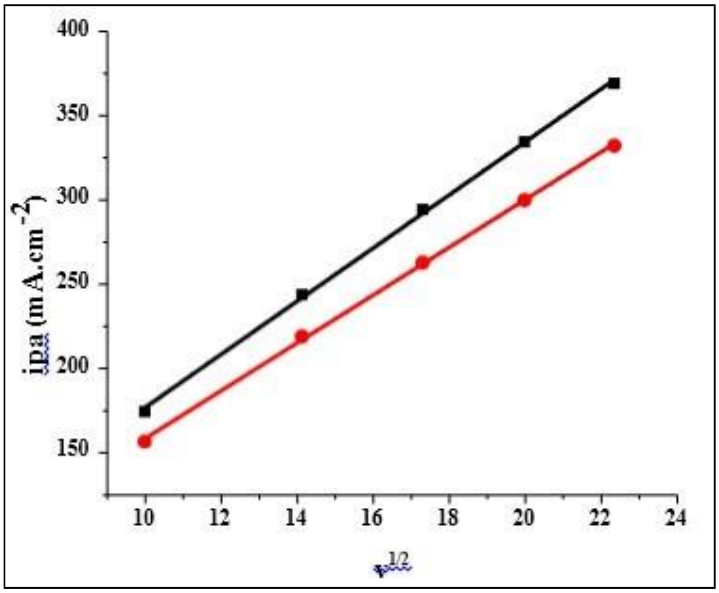

Figure18. Plots of $\sqrt{v}$ versus i_p used to calculate the coefficients diffusion of free and BSA bound forms

Table 12. Diffusion constants values of the free and BSA bound forms

Compound	Equation	R^2	$D(cm^2.s^{-1})$
EO	y = 15.728x + 19.069	0.998	8.099×10^{-7}
EO_BSA	y = 14.1476x + 16.491	0.999	6.549×10^{-7}

The diffusion coefficient of the EO_BSA adducts are lower than is that for the free EO indicating the formation of a high molecular weight complex that diffuses slowly towards the electrode.

5.2. Electronic spectroscopy BSA interaction study:

In order to validate the results obtained from cyclic voltametry techniques and to get complementary method to it, electronic spectroscopy experiments was conducted to study the interaction of *Origanum Majorana L* essential oil with BSA in buffer phosphate solution (KH_2PO_4/K_2HPO_4) at pH = 7.2. The absorption spectra of a fixed concentration (2 mM) of EO in the absence and presence of gradually increasing quantity of BSA stock solution are shown in Figure 19 The studied essential oil showed at one absorption peaks in the visible region. Upon addition of BSA, a significant hyperchromicity was observed without any noticeable shift in the position of maximum absorption peak that clearly indicated the formation of adduct between BSA and the compounds of the EO **(Shah et al., 2010).**

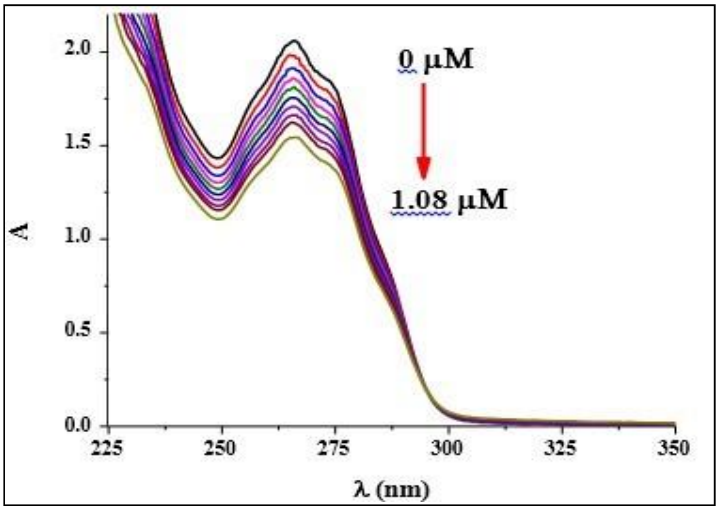

Figure19. UV-visible absorption spectra of 2 mM of *Origanum Majorana L* essential oil in presence of increasing concentrations of BSA in 0.1 M 90% ethanol/buffer phosphate solution (KH_2PO_4/K_2HPO_4) at pH = 7.2 and 298K

5.2.1. Binding constants:

The change in absorbance values by increasing BSA concentration was used to evaluate the intrinsic binding constants and binding free energies using Equation 9 described previously **(Isaac et al., 1999; Ni et al., 1997)**. The constant K_b is obtained from the intercept to slope ratio of the plot of $A_0/(A - A_0)$ versus$1/[BSA]$, Figure 20.

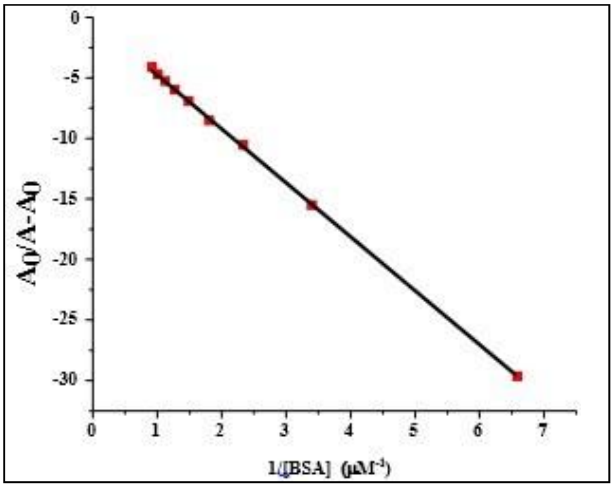

Figure 20. Plots of $\boldsymbol{A_0/(A - A_0)}$ versus $\boldsymbol{1/[BSA]}$ used to calculate the binding constants of essential oil with BSA

5.2.2. Binding free energy:

The binding free energy change was calculated using Equation 10, cited previously. Values are listed in Table 13

Table13. Binding constants and binding free energy changes for the studied essential oil with BSA from UV-Vis data

Adduct	Equation	R^2	K (M^{-1})	-ΔG ($KJ.mol^{-1}$)
EO_BSA	y = -4.48128x - 0.21122	0.99971	4.71×10^5	32.39

5.3. Molecular Docking Study:

Molecular docking was carried out in order to predict the possible binding mode of the identified compounds to BSA and to further visualise the interactions.

Before performing docking calculations, all the crystallographic water molecules were removed from the crystal structure of BSA, hydrogen atoms were added and partial charges were assigned to the BSA structure file. The resulting free binding energy of docked BSA- Ligands adducts are summarised in Table 14

Table 14. Docking score of the studied compounds

Compound	Rigid Docking Score (Kcal/mol)	IFD scores (Kcal/mol)
trans thujone	-6.479	-7.779
cis Verbenyl acetate	-5.854	-7.154
Camphor	-5.415	-6.715
alpha-Thujene	-5.32	-6.62
Sabinene	-5.275	-6.575
Beta Pinene oxide	-5.025	-6.325
alpha-Pinene	-4.794	-6.094
1,8-Cineole	-4.616	-5.916
Santolina triene	-3.896	-5.196

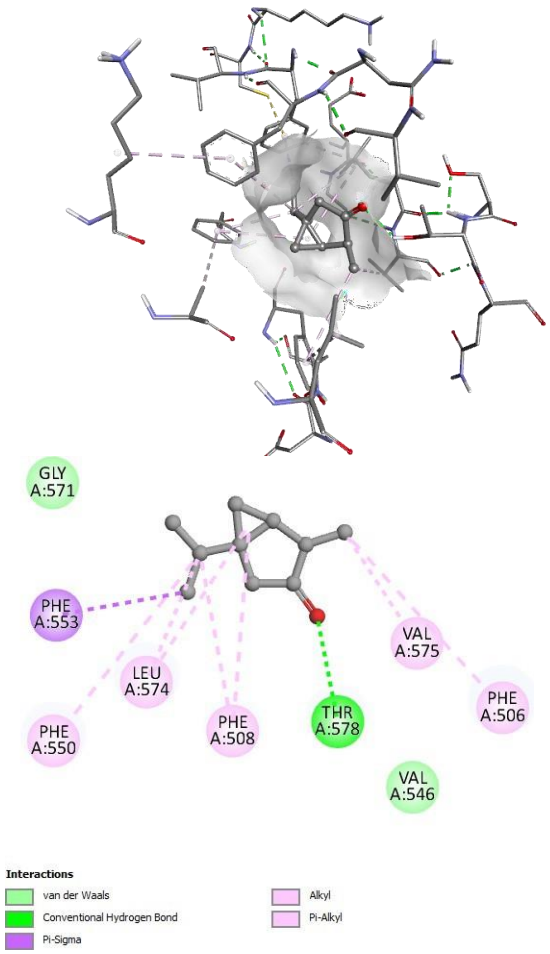

Docking complex and interaction plot for compound trans- thujone with BSA

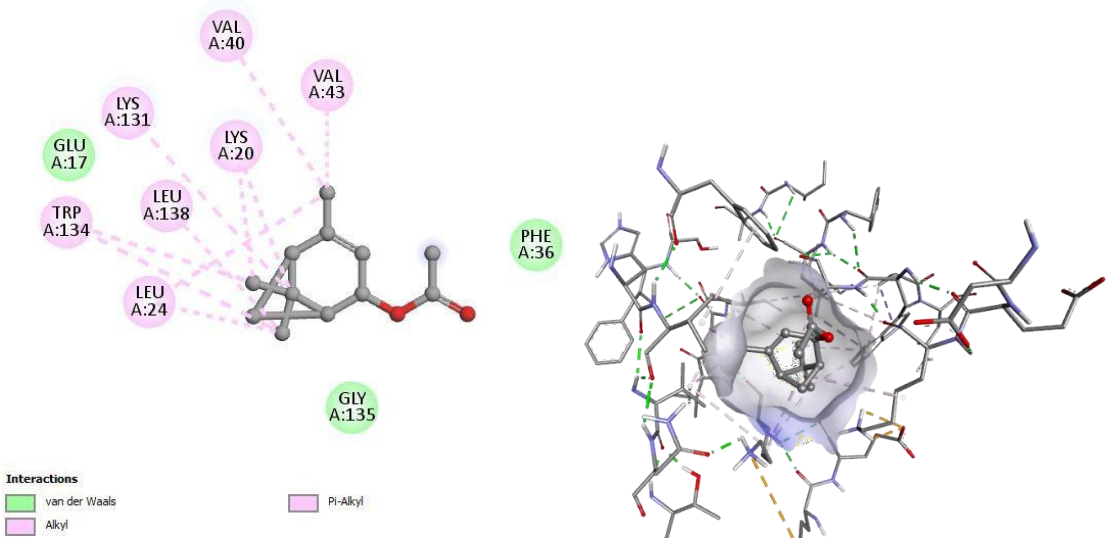

Docking complex and interaction plot for compound cis Verbenyl acetate *with BSA*

Figure 21. Molecular interactions of studied compounds with BSA **(Personal work.,2024)**

6. ADMET and drug-likeness prediction:

Modern drug discovery involves assessment of competence of the dynamic molecules and their strength to reach target site in bioactive form, which involves cellular, animal and human clinical trials which are highly priced and encumbered with risks **(Ranjith & Ravikumar, 2019; Ranjith D & Viswanath S, 2019)**. Presently computer aided drug development encouraged the estimate of absorption, distribution, metabolism and excretion of drugs (ADME), they postulate anticipatory and dependable data very quickly and compliment for experimental approaches **(Ranjith & Ravikumar, 2019; Sliwoski et al., 2014).** It has been determined that the initial appraisal of ADME properties in the discovery period diminishes remarkably the fraction of pharmacokinetics related failures in the clinical phase **(Hay et al., 2014; Ranjith & Ravikumar, 2019).**

In the present study we evaluated the ADME properties of the major compounds (more than 10%) present in the essential oil using SwissADME web tool. A total of 4 potent phytoconstituents were analysed to study general characteristics (Table 15), Physicochemical properties (Table 16), lipophilicity and water solubility characteristics (Table 17 & 18), pharmacokinetic parameters (Table 19), drug likeness rule and bioavailability score (Table 20) and medicinal chemistry properties (Table 21), respectively. General characteristics of the studied compounds revealed all the compounds having molecular weight less than 500 Da, which is a good prime property to be called as drug likeness of the small molecules.

Table15. General characteristics of the phytoconstituents of essential oils

SI. No	Compounds	Molecular formula	Canonical SMILES	Molecular weight (g/mol)
1	Santolina triene	$C_{10}H_{16}$	CC(=CC(C=C)C(=C)C)C	136.23
2	trans-Thujone	$C_{10}H_{16}O$	CC1C2CC2(CC1=O)C(C)C	152.53
3	1,8-Cineole	$C_{10}H_{18}O$	CC1(C2CCC(O1)(CC2)C)C	154.25
4	s-Verbenyl acetate	$C_{12}H_{18}O_2$	C1=CC(C2CC1C2(C)C)OC(=O)C	194.27

Table 16. Physicochemical properties of the phytoconstituents of essential oils

Properties	Santolina triene	trans-Thujone	1,8-Cineole	cis-Verbenyl acetate
Num. heavy atoms	10	11	11	14
Num. arom. heavy atoms	0	0	0	0
Fraction Csp3	0.40	0.90	1.00	0.75
Num. rotatable bonds	3	1	0	2
Num. H-bond acceptors	0	1	1	2
Num. H-bond donors	0	0	0	0
Molar refractivity	48.76	45.90	47.12	56.12
TPSA (Å^2)	0.00	17.07	9.23	26.30

Table17. Lipophilicity characteristics of the phytoconstituents of essential oils

Properties	Santolina triene	trans-Thujone	1,8-Cineole	cis-Verbenyl acetate
iLOGP	2.90	2.27	2.58	2.53
XLOGP3	4.22	2.27	2.74	3.73
WLOGP	3.33	2.26	2.74	2.54
MLOGP	3.56	2.30	2.45	2.65
SILICOS-IT	2.88	2.63	2.86	2.26
Consensus Log Po/w	3.38	2.35	2.67	2.74

Table 18.Water Solubility characteristics of the phytoconstituents of essential oils

Small molecules	SOL				Al				SILICOS-IT			
	Log S (ESOL)	Solubility		Class	Log S (Ali)	Solubility		Class	Log S (SILICOS-IT)	Solubility		Class
		mg/ml	mol/L			mg/ml	mol/L			mg/ml	mol/L	
Santolina triene	-3.15	9.75e-2	7.16e-4	S	-3.93	1.60e-2	1.17e-4	S	-2.04	1.24e-0	9.10e-3	S
trans-Thujone	-2.15	1.08e-0	7.11e-3	S	-2.27	8.27e-1	5.43e-3	S	-2.15	1.08e-0	7.10e-3	S
1,8-Cineole	-2.52	4.63e-1	3.00e-3	S	-2.59	3.98e-1	2.58e-3	S	-2.45	5.45e-1	3.53e-3	S
cis-Verbenyl acetate	-3.26	1.06e-1	5.47e-4	S	-3.97	2.06e-2	1.06e-4	S	-2.11	1.51e-0	7.78e-3	S

Table19. Pharmacokinetics parameters of the phytoconstituents of essential oils

Proprieties	Santolina triene	trans-Thujone	1,8-Cineole	cis-Verbenyl acetate
GI absorption	Low	High	High	Low
BBB permeant	Yes	Yes	Yes	Yes
P-gp substrate	No	No	No	No
CYP1A2 inhibitor	No	No	No	No
CYP2C19 inhibitor	No	No	No	No
CYP2C9 inhibitor	No	No	No	Yes
CYP2D6 inhibitor	No	No	No	No
CYP3A4 inhibitor	No	No	No	No
Log Kp (Skin Permeation) (cm/s)	-4.13	-5.62	-5.30	-4.84

Table 20. Druglikeness rule and bioavailability score of the phytoconstituents of essential oils

Proprieties	Santolina triene	trans-Thujone	1,8-Cineole	cis-Verbenyl acetate
Lipinski	Yes; 0 violations	Yes; 0 violations	Yes; 0 violations	Yes; 0 violations
Ghose	No; 1 violation: MW<160	No; 1 violation: MW<160	No; 1 violation: MW<160	Yes
Veber	Yes	Yes	Yes	Yes
Egan	Yes	Yes	Yes	Yes
Muegge	No; 2 violations: MW<200, XLOGP3>3.5	No; 2 violations: MW<200, Heteroatoms<2	No; 2 violations: MW<200, Heteroatoms<2	No; 1 violation: MW<200,
Bioavailability score	0.55	0.55	0.55	0.55

Table 21. Medicinal Chemistry properties of the Phytoconstituents of essential oils

Proprieties	Santolina triene	trans-Thujone	1,8-Cineole	cis-Verbenyl acetate
PAINS	0 alert	0 alert	0 alert	0 alert
Brenk	1 alert: isolated_alkene	0 alert	0 alert	1 alert: isolated_alkene
Leadlikeness	No; 2 violations: MW<250, XLOGP3>3.5	No; 1 violation: MW<250	No; 1 violation: MW<250	No; 2 violations: MW<250, XLOGP3>3.5
Synthetic accessibility	3.22	2.79	3.65	4.50

Lipophilicity property of the compounds portrays an important role for molecular discovery activities in multifarious domains. The quantitative descriptor of the lipophilicity is the partition coefficient P of a given molecule between *n*-octanol and water system (Daina et al., 2014). Because of its amphiphilic nature, *n*-octanol is considered a good mimic of phospholipid membrane characteristics (Liu et al., 2011). Multifarious algorithms are accessible to compute log Po/w, which rely on factual methodologies. The classic log P predictors branched in to two division, first ones split molecular structures into molecular fragments includes fragmental approach e.g. KLOGP (Klopman et al., 1993), KOWWNIN (Meylan & Howard, 2000) or atomic approach e.g. ALOGP (Ghose et al., 1998; R. Wang et al., 1997), XLOGP (Cheng et al., 2007; Moriguchi et al., 1994). The second division gathers the topological methods in which, the molecules description is related to its topology being as count or flags for specific atoms, groups or structural properties e.g. MLOGP (Brenk et al., 2008; Moriguchi et al., 1992), the prediction attained by manifold linear regression trained on large molecular data sets. The SILICOS-IT is a hybrid technique which combines both molecular fragments and topological parameters, which confide on 27 fragments and 7 topological descriptors, it was disciplined on 23,455 molecules with experimental *n*-octanol/water partition values (Daina et al., 2014). The version three of the XLOGP atomic model is established on a system of 87 fragments and two corrective factors. If the input structures are similar to a reference compound, the fragments differentiating them are treated and the corresponding log P contributions added to the reference structure log P value (Cheng et al., 2007). Lipophilicity estimated as consensus Log P, which is the average value of all Log P evaluated with various lipophilicity criteria, determined 1,8- Cineol as most lipophilic whereas santolina triene as least lipophilic and water solubility of the small molecules ranged from highly water soluble to water soluble.

The SwissADME model returns “Yes” or “No” if the compound under examination has greater probability to be a substrate or non-substrate of P-gp or inhibitor or non-inhibitor of Cytochrome P450 isoenzymes (CYP1A2, CYP2C9, CYP2C19, CYP2D6 and CYP3A4).

The pharmacokinetics and drug likeness performed using SwissADME showed a low level of GI absorption and BBB permeant with santolina triene and cis-Verbenyl acetate while a high absorption detected with trans-Thujone and 1,8-Cineole. All the compounds present in the essential oils are not the substrates for P-gp (Table 19), so they are not susceptible to the efflux mechanism performed by this transporter which is used by many tumours cell lines as a drug- resistance mechanism (Ranjith & Ravikumar, 2019)

All of the small molecules returned as non-inhibitors for inactivation for CYP isoenzymes. The skin permeability coefficient (Log Kp), a multiple linear regression, the more negative the

log Kp (with Kp in cm/s), the less skin permeant is the molecule. Among the phytoconstituents, trans-Thujone (-5.62) is the least permeant and santolina triene (-4.13) is highly permeant respectively. This SwissADME section gives access to five different rule-based filters, with diverse ranges of properties inside of which the molecule is defined as drug-like. The Lipinski (Pfizer) filter is the pioneer rule-of-five implemented and with the Ghose (Amgen), Veber (GSK), Egan (Pharmacia) and Muegge (Bayer) methods. Multiple estimations allow consensus views or selection of methods best fitting the end-user's specific needs in terms of chemical space or project-related demands. Any violation of any rule described here appears explicitly in the output panel. All the four compounds followed the filtered rule invoked in the SwissADME; the violation shown by the molecules are minimal.

SwissADME interpretation posts 0 PAINS alert of the 4 studied compounds. Brenk considered compounds that are smaller and less hydrophobic and not those defined by "Lipinski's rule of 5" to widen opportunities for lead optimization. This was after exclusion of compounds with potentially mutagenic, reactive and unfavourable groups such as nitro groups, sulphates, phosphates, 2-halopyridines and thiols (Brenk et al., 2008). All the compounds examined flouted Brenk's rule with only one alert, all the compounds failed Lead-likeness criteria due to their molar weight.

In silico toxicity study aims to help in optimizing compounds regarding their toxicity proprieties. The study could offer an important improvement to the awareness of the full perspective of virtual screening for the identification of target compounds with negligible or no toxicity, which may open a path for the selection of novel nontoxic phytoconstituents present in *Origanum Majorana L* essential oils with high antidiabetic activity. In silico toxicity study of the chosen compounds was performed using the ProTox-II web server (Drwal et al., 2014). It aims to predict hepatotoxicity (Dili), carcinogenicity (Carcino), immunotoxicity (Immuno), mutagenicity (Mutagen), cytotoxicity (Cyto), median lethal dose (LD50), and toxicity class (TC).

According to in silico toxicity profiles presented in Table 22. the toxicity class of all the phytoconstituents was detected to be equal to 5 except the trans-Thujone which predicted to be

4. Santolina triene, trans-Thujone**,** 1,8-Cineole and cis-Verbenyl acetate were predicted to be nontoxic except in immunotoxicity for the last wrote compound.

Table 22. In silico toxicity profiles of the studied compounds

Molecule	Dili	Carcino	Immuno	Mutagen	Cyto	LD_{50} (mg.Kg^{-1})	TC
Santolina triene	Inactive	Active	Inactive	Inactive	Inactive	2610	5
trans-Thujone	Inactive	Inactive	Inactive	Inactive	Inactive	500	4
1,8-Cineole	Inactive	Inactive	Inactive	Inactive	Inactive	2480	5
cis-Verbenyl acetate	Inactive	Inactive	Active	Inactive	Inactive	2600	5

1. Molecular Dynamics Simulation:

Molecular Dynamics Simulation (MDS) investigations were conducted for the premier compound show the best IFD score, trans- thujone, in complex with BSA. The principal objective of these MDS endeavours was to subject the ligand-receptor complex to physiological conditions, a feat unattainable through the confines of molecular docking (Dumitrică & James, 2007). Throughout the MDS protocol, a trajectory frame was generated at intervals of 100 picoseconds (Tu et al., 2008), accumulating a total of 1000 frames over the course of a 100- nanosecond simulation. Analysis encompassed metrics such as 'Root Mean Square Deviation (RMSD), and 'Root Mean Square Fluctuation (RMSF). Specifically, RMSD values were computed by aligning the frames of the protein and ligand-protein complex with the reference frame, respectively. These analytical approaches provide a detailed understanding of the structural stability and dynamic fluctuations exhibited by the Ligand-BSA complex throughout the simulation period (Schreiner et al., 2012).

The Root Mean Square Deviation (RMSD) values for the complex consistently fall within the acceptable range of 0 – 2 Å. Examination of the analysed complex revealed no significant conformational alterations; however, an initial minor deviation was discerned in the vicinity of

8 – 20 nanoseconds, and a subtle drift was observed approximately between 45 – 55 nanoseconds. Beyond these periods, the complex demonstrated marked stability throughout the entirety of the simulation process, with no notable occurrence of major conformational changes. (Figure 22).

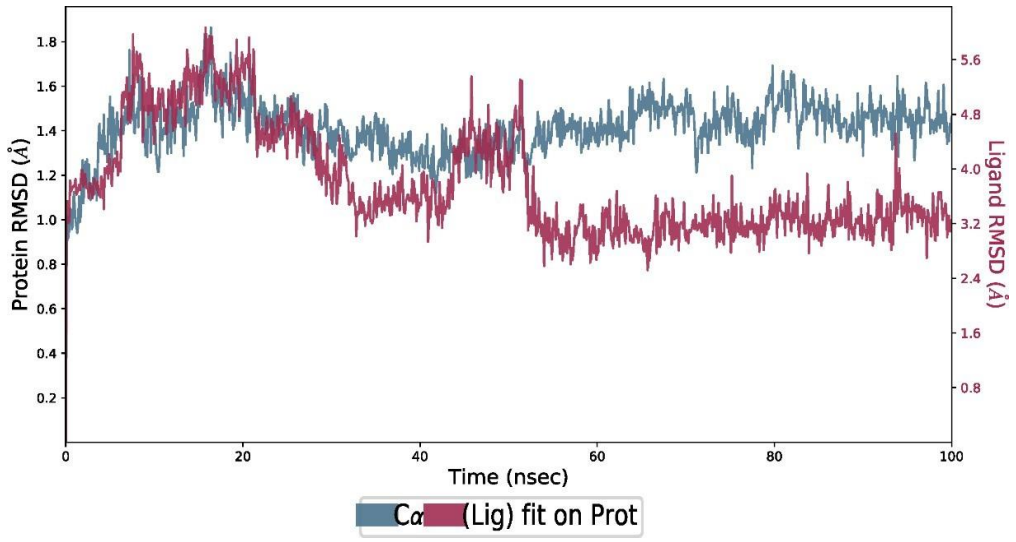

Figure22. RMSD plot of trans- thujone and BSA complex

The Root Mean Square Fluctuation (RMSF) analysis provides insights into local variations along the protein chain, facilitating the identification of residues contributing to structural fluctuations within the complex (Dey et al., 2021). In the examined complex, the observed fluctuation variation remained below 3 Å. Major fluctuations (2.20-2.63 and 1.81-2.96Å) were observed in the C-terminal and loop regions (223-225 and 363-366), respectively, which are positioned away from the binding pocket of BSA. Except for the loop regions, the RMSF values of most residues are less than 1.5 Å, indicating that the residue conformation is relatively stable during the simulation. A graphical representation of the RMSF plot depicting the specific ligand interactions with amino acid residues in the protein is presented in Figure 23.

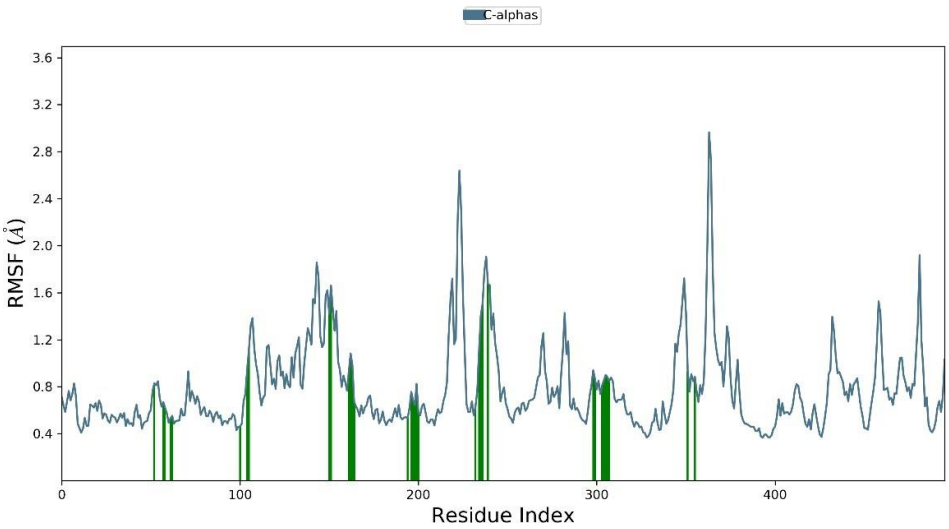

Figure23. RMSF plot of trans- thujone and BSA complex

Within the investigated complex, notable hydrogen bond interactions were observed involving HIS299, ASP197, and TRP58. Additionally, water-mediated hydrogen bond interactions were formed, encompassing the same residues, as visually depicted in Figure 24.

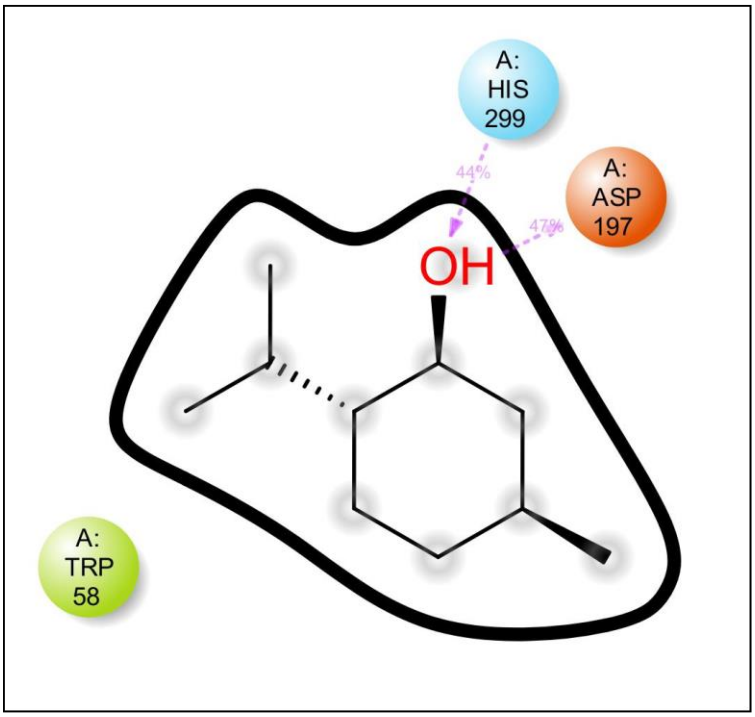

Figure 24. Interaction diagram of protein-ligand after MDS

The analysis of Protein-ligand contact serves to elucidate the temporal continuity of interactions between the ligand and protein amino acids throughout the simulation. A numerical representation is employed, where a value of 0.5 denotes that a specific interaction was sustained for 50% of the simulation duration. Conversely, a value exceeding 1 suggests that protein amino acids may establish multiple contacts of the same subtype with the ligand (Hatmal & Taha, 2017).

In the context of the investigated complex, the interaction values for the residues GLU240, HIS201, ASP197, GLN63, GLU233, and THR163 are recorded as 1.25, 1, 1.75, 1, 0.60, and

1.5, respectively. These values signify varying degrees of sustained interactions between the ligand and corresponding amino acid residues. The graphical representation of the protein-ligand contact histograms for the complex is depicted in Figure 25 for visual elucidation.

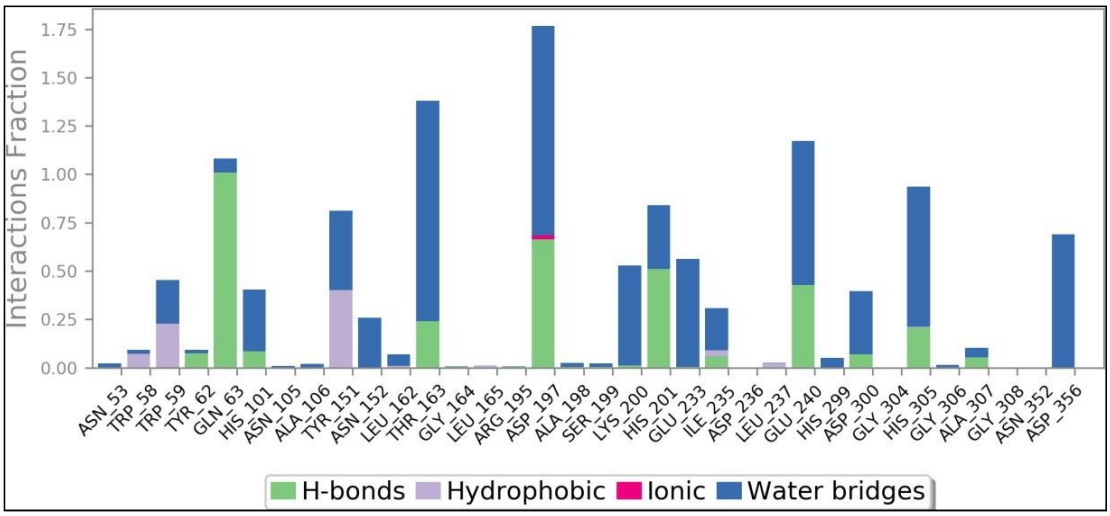

Figure25.. Histogram of protein-ligand complex

To comprehensively investigate the interactions between the ligand and BSA receptor, two supplementary panels were introduced by Schrödinger post Molecular Dynamics Simulation (MDS), as depicted in Figure 26. The upper panel provides insights into the total number of specific contacts established by the protein with the ligand throughout the trajectory. Conversely, the lower panel delineates the residues engaged in interactions with the ligand in each trajectory frame.

Notably, certain residues exhibit multiple specific contacts with the ligand, visualized through varying shades of orange on the plot, in accordance with the scale positioned to the right of the diagram. This nuanced representation captures the dynamic nature of the interactions, offering a detailed portrayal of the residues that consistently contribute to the ligand-receptor interface. The incorporation of these supplementary panels enhances the granularity of our understanding of the molecular dynamics and specific contacts governing the ligand-receptor interaction over the course of the simulation.

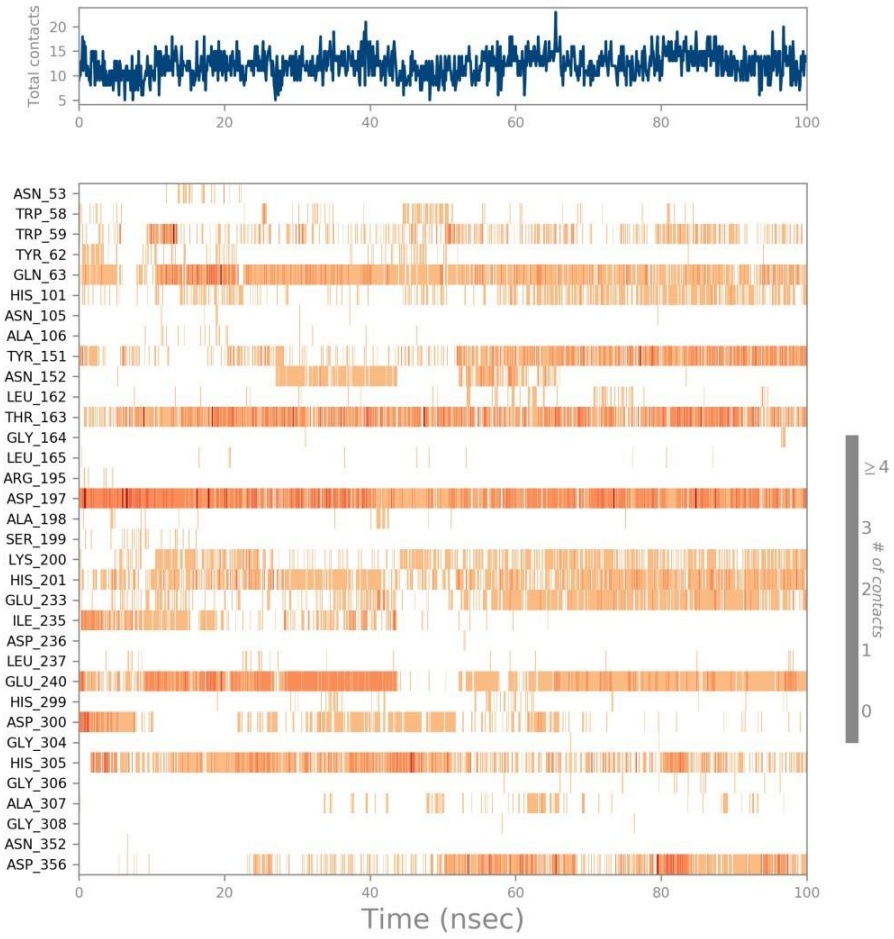

Figure 26. Details of the protein ligand contact

2. Free Energy (MM-GBSA) Calculation:

To evaluate the binding efficacy of the preeminent compound, trans- thujone, with the BSA protein, the Prime-MM-GBSA method was applied to compute the binding free energies. The establishment of stable complexes is evidenced by favourable binding interactions between the compound and the protein. The determination of binding free energy entails the consideration of various energy components, encompassing van der Waals (vdW), lipophilic (lipo), Generalized Born electrostatic solvation (Solv GB), Coulomb, and hydrogen-bonding (hbond) energies. The discrete contributions of these energy components to the overall binding free energy of the trans-thujone -BSA complex are delineated in Table 23.

Table 23. Energy components of the studied complex

Component	Energy (kcal/mol)
ΔG Bind	-61.14
ΔG Bind Coulomb	-30.03
ΔG Bind Solv GB	48.10
ΔG Bind vdW	-54.91
ΔG Bind lipo	-20.51
ΔG Bind hbond	-3.79

Notably, ΔG Bind is calculated at -61.14 kcal/mol, indicating a robust favourable binding interaction. Individual positive contributions include Coulombic energy at -30.03 kcal/mol, van der Waals interactions at -54.91 kcal/mol, lipophilic energy at -20.51 kcal/mol, and hydrogen-bonding energy at -3.79 kcal/mol. However, solvation energy through Generalized Born model contributed negatively at 48.10 kcal/mol. This collective interplay of energy components underscores the strong binding affinity observed in the complex.

CONCLUSION

Conclusion

This thesis focused on the biological activity of *Origanum Majorana L* essential oil in the laboratory, in addition to predicting its behavior within the silico through molecular docking and molecular dynamics. The results revealed that this oil possesses several intriguing biological activities, in- cluding anticancer properties, making it a valuable compound in medicine and pharmacology. La- boratory tests indicated that wild thyme oil exhibits significant anticancer activity against breast, lung, and prostate cancer cells. This anticancer activity of the oil was observed with both DNA and BSA protein. These results suggest that wild thyme oil has significant therapeutic potential for treating various diseases.

Molecular docking and molecular dynamics simulations in silico confirmed the laboratory test results by demonstrating that wild thyme oil binds to active sites of certain cancer-related enzymes. Additionally, molecular dynamics simulations showed that ligand- protein complexes remained stable throughout the simulation period.

Toxicity predictions indicated that wild thyme oil has low toxicity, supporting its potential as a therapeutic compound. The findings of this study may help guide future research on the use of this oil as a potential drug for treating various diseases.

REFERENCES

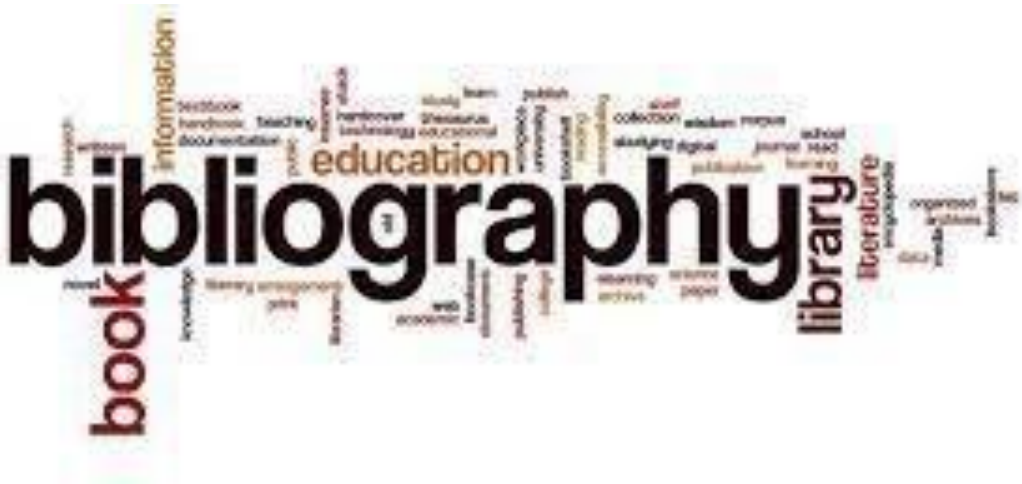
bibliography
education
information
book
library
literature

References bibliography

- Afnor, Ø. (1982). Recueil de normes françaises des produits dérivés des fruits et légumes jus de fruits. *AFNOR*, *325*.
- Akbar, S., Das, S., Iqubal, A., & Ahmed, B. (2022). Synthesis, biological evaluation and molecular dynamics studies of oxadiazine derivatives as potential anti-hepatotoxic agents. *Journal of Biomolecular Structure and Dynamics*, *40*(20), 9974–9991. https://doi.org/10.1080/07391102.2021.1938233
- Alajtal, A. I., Sherami, F. E., & Elbagermi, M. A. (2018). Acid, peroxide, ester and saponification values for some vegetable oils before and after frying. *AASCIT Journal of Materials*, *4*(2), 43–47.
- Ali, S., Altaf, A. A., Badshah, A., Lal, B., Kamal, S., & Ullah, S. (2013). DNA interaction, Antibacterial and Antifungal studies of 3-nitrophenylferrocene. *Journal of the Chemical Society of Pakistan*, *34*(3).
- Alimi, D., Hajri, A., Jallouli, S., & Sebai, H. (2022). Valorization of Volatile Oils and Some Crude Extracts from the Tunisian Plants Juniperus communis and Origanum majorana for the Control of Hyalomma scupense (Acari: Ixodidae). *Waste and Biomass Valorization*, *13*(10), 4165–4177.
- Atti-Santos, A. C., Rossato, M., Pauletti, G. F., Rota, L. D., Rech, J. C., Pansera, M. R., Agostini, F., Serafini, L. A., & Moyna, P. (2005). Physico-chemical evaluation of Rosmarinus officinalis L. essential oils. *Brazilian Archives of Biology and Technology*, *48*, 1035–1039.
- Avwioroko, O. J., Oyetunde, T. T., Atanu, F. O., Otuechere, C. A., Anigboro, A. A., Dairo, O. F., Ejoh, A. S., Ajibade, S. O., & Omorogie, M. O. (2020). Exploring the binding interactions of structurally diverse dichalcogenoimidodiphosphinate ligands with α- amylase: Spectroscopic approach coupled with molecular docking. *Biochemistry and Biophysics Reports*, *24*, 100837. https://doi.org/10.1016/j.bbrep.2020.100837
- Banerjee, P., Eckert, A. O., Schrey, A. K., & Preissner, R. (2018). ProTox-II: A webserver for the prediction of toxicity of chemicals. *Nucleic Acids Research*, *46*(W1), W257–W263. https://doi.org/10.1093/nar/gky318
- Baser, K. H. C., Kirimer, N., & Tümen, G. (1993). Composition of the essential oil of Origanum majorana L. from Turkey. *Journal of Essential Oil Research*, *5*(5), 577–579.
- Biswa, M. S., Varsha, T., Abhishek, T., & Bimal, K. B. (2023). Green Chemistry using

- Essential Oils as Synthons. *Journal of Indian Chemical Society*, *Mar2023*, 1–24. https://doi.org/10.5281/zenodo.7841465
- Bowers, K. J., Chow, E., Xu, H., Dror, R. O., Eastwood, M. P., Gregersen, B. A., Klepeis, J. L., Kolossvary, I., Moraes, M. A., & Sacerdoti, F. D. (2006). Scalable algorithms for molecular dynamics simulations on commodity clusters. *Proceedings of the 2006 ACM/IEEE Conference on Supercomputing*, 84-es.
- Brenk, R., Schipani, A., James, D., Krasowski, A., Gilbert, I. H., Frearson, J., & Wyatt, P. G. (2008). Lessons learnt from assembling screening libraries for drug discovery for neglected diseases. *ChemMedChem*, *3*(3), 435–444. https://doi.org/10.1002/cmdc.200700139
- Castagna, R., Donini, S., Colnago, P., Serafini, A., Parisini, E., & Bertarelli, C. (2019). Biohybrid Electrospun Membrane for the Filtration of Ketoprofen Drug from Water. *ACS Omega*, *4*(8), 13270–13278. https://doi.org/10.1021/acsomega.9b01442
- Cheng, T., Zhao, Y., Li, X., Lin, F., Xu, Y., Zhang, X., Li, Y., Wang, R., & Lai, L. (2007). Computation of octanol-water partition coefficients by guiding an additive model with knowledge. *Journal of Chemical Information and Modeling*, *47*(6), 2140–2148. https://doi.org/10.1021/ci700257y
- Chiu, S. Y. C., Dobberstein, R. H., Fong, H. H. S., & Farnsworth, N. R. (1982). Oxoaporphine alkaloids from Siparuna gilgiana. *Journal of Natural Products*, *45*(2), 229–230.
- Court, R., Chapman, L., Fairall, L., & Rhodes, D. (2005). How the human telomeric proteins TRF1 and TRF2 recognize telomeric DNA: A view from high-resolution crystal structures. *EMBO Reports*, *6*(1), 39–45. https://doi.org/10.1038/sj.embor.7400314
- Daina, A., Michielin, O., & Zoete, V. (2014). ILOGP: A simple, robust, and efficient description of n-octanol/water partition coefficient for drug design using the GB/SA approach. *Journal of Chemical Information and Modeling*, *54*(12), 3284–3301. https://doi.org/10.1021/ci500467k
- Daina, A., Michielin, O., & Zoete, V. (2017). SwissADME: A free web tool to evaluate pharmacokinetics, drug-likeness and medicinal chemistry friendliness of small molecules. *Scientific Reports*, *7*(1), 1–13. https://doi.org/10.1038/srep42717
- Dey, D., Paul, P. K., Azad, S. Al, Mazid, M. F. Al, Khan, A. M., Sharif, M. A., & Rah-

man, M. H. (2021). Molecular optimization, docking, and dynamic simulation profiling

- of selective aromatic phytochemical ligands in blocking the SARS-CoV-2 S protein attachment to ACE2 receptor: an in silico approach of targeted drug designing. *Journal of Advanced Veterinary and Animal Research*, *8*(1), 24–35.
- https://doi.org/10.5455/javar.2021.h481
- Drwal, M. N., Banerjee, P., Dunkel, M., Wettig, M. R., & Preissner, R. (2014). ProTox: A web server for the in silico prediction of rodent oral toxicity. *Nucleic Acids Research*, *42*(W1), W53–W58. https://doi.org/10.1093/nar/gku401
- Dumitrică, T., & James, R. D. (2007). Objective molecular dynamics. *Journal of the Mechanics and Physics of Solids*, *55*(10), 2206–2236. https://doi.org/10.1016/j.jmps.2007.03.001
- El-Hallag, I. S. (2010). Electrochemical oxidation of iodide at a glassy carbon electrode in methylene chloride at various temperatures. *Journal of the Chilean Chemical Society*, *55*(1), 67–73. https://doi.org/10.4067/S0717-97072010000100016
- Filote, C., Lanez, E., Popa, V. I., Lanez, T., & Volf, I. (2022). Characterization and Bioactivity of Polysaccharides Separated through a (Sequential) Biorefinery Process from Fucus spiralis Brown Macroalgae. *Polymers*, *14*(19), 4106.
- https://doi.org/10.3390/polym14194106
- French, J. B., Neau, D. B., & Ealick, S. E. (2011). Characterization of the Structure and Function of Klebsiella pneumoniae Allantoin Racemase. *Journal of Molecular Biology*, *410*(3), 447–460. https://doi.org/https://doi.org/10.1016/j.jmb.2011.05.016
- Friesner, R. A., Murphy, R. B., Repasky, M. P., Frye, L. L., Greenwood, J. R., Halgren, T. A., Sanschagrin, P. C., & Mainz, D. T. (2006). Extra precision glide: Docking and scoring incorporating a model of hydrophobic enclosure for protein−ligand complexes. *Journal of Medicinal Chemistry*, *49*(21), 6177–6196.
- Gaaib, J. N., Nassief, A. F., & Al-assi, A. H. (2011). Simple salting – out method for genomic DNA extraction from whole blood Abstract : Introduction : *Nucleic Acids Research*, *16*(2), 15–17.
- Gharagozlou, M., & Boghaei, D. M. (2008). Interaction of water-soluble amino acid
- Schiff base complexes with bovine serum albumin: fluorescence and circular dichroism studies. *Spectrochimica Acta Part A: Molecular and Biomolecular Spec-*

troscopy, *71*(4), 1617– 1622.

- Ghose, A. K., Viswanadhan, V. N., & Wendoloski, J. J. (1998). Prediction of hydrophobic (lipophilic) properties of small organic molecules using fragmental methods: An analysis of ALOGP and CLOGP methods. *Journal of Physical Chemistry A*, *102*(21), 3762–3772. https://doi.org/10.1021/jp980230o
- Gorla, U. S., Gsn, K. R., Kulandaivelu, U., Alavala, R. R., Das, S., & Joseph, A. (2021). Bioflavonoids as potential target inhibitors in covid-19: An in silico analysis. *Journal of Research in Pharmacy*, *25*(6), 982–997. https://doi.org/10.29228/jrp.94
- Griffiths, L., & Chacon-Cortes, D. (2014). Methods for extracting genomic DNA from whole blood samples: current perspectives. *Journal of Biorepository Science for Applied*

- *Medicine*, *2014*(2), 1. https://doi.org/10.2147/bsam.s46573
- Guinaudeau, H., Leboeuf, M., & Cave, A. (1975). *Aporphine alkaloids.*
- Guo, Y.-J., Chao, J.-B., & Pan, J.-H. (2007). Study on the interaction of 5-pyridine-10, 15, 20- tris-(p-chlorophenyl) porphyrin with cyclodextrins an DNA by spectroscopy.
- *Spectrochimica Acta Part A: Molecular and Biomolecular Spectroscopy*, *68*(2), 231–236. Halder, D., Das, S., Joseph, A., & Jeyaprakash, R. S. (2023). Molecular docking and dynamics approach to in silico drug repurposing for inflammatory bowels disease by targeting TNF alpha. *Journal of Biomolecular Structure and Dynamics*, *41*(8)3462–3475.https://doi.org/10.1080/07391102.2022.2050948

- Hatmal, M. M., & Taha, M. O. (2017). Simulated annealing molecular dynamics and ligand- receptor contacts analysis for pharmacophore modeling. *Future Medicinal Chemistry*, *9*(11), 1141–1159. https://doi.org/10.4155/fmc-2017-0061
- Hay, M., Thomas, D. W., Craighead, J. L., Economides, C., & Rosenthal, J. (2014). Clinical development success rates for investigational drugs. *Nature Biotechnology*, *32*(1), 40–51. https://doi.org/10.1038/nbt.2786
- Heckel, R., Shomorony, I., Ramchandran, K., & Tse, D. N. C. (2017). Fundamental limits of DNA storage systems. *IEEE International Symposium on Information Theory - Proceedings*, 3130–3134. https://doi.org/10.1109/ISIT.2017.8007106
- Horai, H., Arita, M., Kanaya, S., Nihei, Y., Ikeda, T., Suwa, K., Ojima, Y., Tanaka, K., Tanaka, S., & Aoshima, K. (2010). MassBank: a public repository for sharing

mass spectral data for life sciences. *Journal of Mass Spectrometry*, *45*(7), 703–714.

- Howe, J. R. (1997). DNA extraction from paraffin-embedded tissues using a salt- ing-out procedure: A reliable method for PCR amplification of archival material. *Histology and Histopathology*, *12*(3), 595–601.
- Husain, M. A., Sarwar, T., Rehman, S. U., Ishqi, H. M., & Tabish, M. (2015). Ibuprofen causes photocleavage through ROS generation and intercalates with DNA: a combined biophysical and molecular docking approach. *Physical Chemistry Chemical Physics*, *17*(21), 13837–13850.
- Isaac, C., Gibson, A., Horrocks, B., & Elsegood, M. J. (1999). Synthesis, structure and redox properties of ferrocenylmethylnucleobases. *Journal of the Chemical Society, Dalton Transactions*, *18*, 3229–3234.
- Jamil, M., Altaf, A. A., Badshah, A., Ahmad, I., Zubair, M., Kemal, S., & Ali, M. I. (2013). Naked Eye DNA detection: Synthesis, characterization and DNA binding studies of a novel azo-guanidine. *Spectrochimica Acta Part A: Molecular and Biomolecular Spectroscopy*, *105*, 165–170.
- Javanrouh, A., & Jelokhani-niaraki, S. (2020). DNA extraction from chicken blood using a modified Salting-out method. *Applied Animal Science Research Journal*, *9*(34), 3–10.
- Khelil, C. K. M., Amrouche, B., soufiane Benyoucef, A., Kara, K., & Chouder, A. (2020). New Intelligent Fault Diagnosis (IFD) approach for grid-connected photovoltaic systems. *Energy*, *211*, 118591.
- Khennoufa, A., Bechki, L., Lanez, T., Lanez, E., & Zegheb, N. (2021). Spectrophotometric, voltammetric and molecular docking studies of binding interaction of N-ferrocenylmethylnitroanilines with bovine serum albumin. *Journal of Molecular Structure*, *1224*, 129052. https://doi.org/10.1016/j.molstruc.2020.129052
- Kim, S., Thiessen, P. A., Bolton, E. E., Chen, J., Fu, G., Gindulyte, A., Han, L., He, J., He, S., Shoemaker, B. A., Wang, J., Yu, B., Zhang, J., & Bryant, S. H. (2016). PubChem substance and compound databases. *Nucleic Acids Research*, *44*(D1), D1202–D1213. https://doi.org/10.1093/nar/gkv951
- Kiryakov, H. G. (1968). *Structure of dehydroglaucine: a new aporphine alkaloid.*
- Klopman, G., Li, J. Y., Wang, S., & Dimayuga, M. (1993). Computer automated log P calculations based on an extended group contribution approach. *Journal of Chemical Information and Computer Sciences*, *33*(4), 752–781.

- Korb, O., Olsson, T. S. G., Bowden, S. J., Hall, R. J., Verdonk, M. L., Liebeschuetz, J. W., & Cole, J. C. (2012). Potential and limitations of ensemble docking. *Journal of Chemical Information and Modeling*, *52*(5), 1262–1274.
- Lanez, E., Bechki, L., & Lanez, T. (2019). Computational molecular docking, voltammetric and spectroscopic DNA interaction studies of 9N-(Ferrocenylmethyl)adenine. *Chemistry and Chemical Technology*, *13*(1), 11–17. https://doi.org/10.23939/chcht13.01.011
- Lanez, T., & Hemmami, H. (2016). Antioxidant Activities of N-ferrocenylmethyl-2- and -3- nitroaniline and Determination of their Binding Parameters with Superoxide Anion Radicals. *Current Pharmaceutical Analysis*, *13*(2), 110–116. https://doi.org/10.2174/1573412912666160831145524
- Lanez, T., Henni, M., & Hemmami, H. (2015). Development of cyclic voltammetric method for the study of the interaction of antioxidant standards with superoxide anion radicals case of α-tocopherol. *Scientific Study and Research: Chemistry and Chemical Engineering, Biotechnology, Food Industry*, *16*(2), 161–168.
- Larbi, B. A. M., Naima, B., Elsharkawy, E. R., & Neghmouche, N. S. (2018). Phytochemical characterization, in-vitro cytotoxic and antibacterial activity of Cotula cinerea (Delile) Vis essential oil. *Journal of Natural Remedies*, 107–112.
- Liu, X., Testa, B., & Fahr, A. (2011). Lipophilicity and its relationship with passive drug permeation. *Pharmaceutical Research*, *28*(5), 962–977. https://doi.org/10.1007/s11095-
- 010-0303-7
- Lu, C., Wu, C., Ghoreishi, D., Chen, W., Wang, L., Damm, W., Ross, G. A., Dahlgren, M. K., Russell, E., & Von Bargen, C. D. (2021). OPLS4: Improving force field accuracy on challenging regimes of chemical space. *Journal of Chemical Theory and Computation*, *17*(7), 4291–4300.
- Madhavi Sastry, G., Adzhigirey, M., Day, T., Annabhimoju, R., & Sherman, W. (2013). Protein and ligand preparation: parameters, protocols, and influence on virtual screening enrichments. *Journal of Computer-Aided Molecular Design*, *27*, 221–234.
- Meylan, W. M., & Howard, P. H. (2000). Estimating log P with atom/fragments and water solubility with log P. *Perspectives in Drug Discovery and Design*, *19*(1), 67–84. https://doi.org/10.1023/A:1008715521862

- Miller, S. A., Dykes, D. D., & Polesky, H. F. (1988). A simple salting out procedure for extracting DNA from human nucleated cells. *Nucleic Acids Research*, *16*(3), 1215. https://doi.org/10.1093/nar/16.3.1215
- Moriguchi, I., Hirano, H., & Nakagome, I. (1994). Comparison of Reliability of log P Values for Drugs Calculated by Several Methods. *Chemical and Pharmaceutical Bulletin*, *42*(4), 976–978. https://doi.org/10.1248/cpb.42.976
- Moriguchi, I., Hirono, S., Liu, Q., Nakagome, Izum., & Matsushita, Y. (1992). Simple Method of Calculating Octanol/Water Partition Coefficient. *Chemical and Pharmaceutical Bulletin*, *40*(1), 127–130. https://doi.org/10.1248/cpb.40.127
- Moriuchi, T., Bandoh, S., Miyaji, Y., & Hirao, T. (2000). A novel heterobimetallic complex composed of the imide-bridged [3] ferrocenophane and the tridentate palladium (II) complex. *Journal of Organometallic Chemistry*, *599*(2), 135–142.
- Mouada, H., Lanez, T., & Lanez, E. (2019). Investigations of the binding parametres of the interaction of N'-ferrocenylmethyl-N'-phenylaceto-and propionohydrazide with DNA. *Journal of Fundamental and Applied Sciences*, *11*(2), 875–882.
- Naima, B., Abdelkrim, R., Ouarda, B., Salah, N. N., & Larbi, B. A. M. (2019). Chemical composition, antimicrobial, antioxidant and anticancer activities of essential oil from Ammodaucus leucotrichus Cosson & Durieu (Apiaceae) growing in South Algeria. *Bulletin of the Chemical Society of Ethiopia*, *33*(3), 541–549.
- Narramore, S., Stevenson, C. E. M., Maxwell, A., Lawson, D. M., & Fishwick, C. W. G. (2019). New insights into the binding mode of pyridine-3-carboxamide inhibitors of E. coli DNA gyrase. *Bioorganic and Medicinal Chemistry*, *27*(16), 3546–3550. https://doi.org/10.1016/j.bmc.2019.06.015
- Nasiri, H., Forouzandeh, M., Rasaee, M. J., & Rahbarizadeh, F. (2005). Modified salting-out method: High-yield, high-quality genomic DNA extraction from whole blood using laundry detergent. *Journal of Clinical Laboratory Analysis*, *19*(6), 229–232. https://doi.org/10.1002/jcla.20083
- Ni, M. Y., Wang, Y., & Li, H. L. (1997). Electrochemical and spectral properties of phenylhydrazine in the presence of β-cyclodextrin. *Pol. J. Chem.*, *71*, 816–822.
- Ning, J., Liebich, J., Kästner, M., Zhou, J., Schäffer, A., & Burauel, P. (2009). Different influences of DNA purity indices and quantity on PCR-based DGGE and functional gene microarray in soil microbial community study. *Applied Microbiology and Biotechnology*, *82*(5), 983–993. https://doi.org/10.1007/s00253-009-1912-0

- Oliva, M. A., Trambaiolo, D., & Löwe, J. (2007). Structural Insights into the Conformational Variability of FtsZ. *Journal of Molecular Biology*, *373*(5), 1229–1242. https://doi.org/https://doi.org/10.1016/j.jmb.2007.08.056
- Rakesh, K. P., Shiva Prasad, K., & Shridhara Prasad, K. (2012). Synthesis and characterization of chromium (III) complexes of 4 (3H)-quinazolinone derived schiff base: antimicrobial and DNA interaction studies. *Int. J. Res. Chem. Environ*, *2*, 221–225.
- Ranjith, D., & Ravikumar, C. (2019). SwissADME predictions of pharmacokinetics and drug- likeness properties of small molecules present in Ipomoea mauritiana Jacq. *Journal of Pharmacognosy and Phytochemistry*, *8*(5), 2063–2073.
- Ranjith D, & Viswanath S. (2019). In silico antidiabetic activity of bioactive compounds in Ipomoea mauritiana Jacq. *~ 5 ~ The Pharma Innovation Journal*, *8*(10), 5–11. http://www.thepharmajournal.com
- Rivero, E. R. C., Neves, A. C., Silva-Valenzuela, M. G., Sousa, S. O. M., & Nunes, F. D. (2006). Simple salting-out method for DNA extraction from formalin-fixed, paraffin-embedded tissues. *Pathology-Research and Practice*, *202*(7), 523–529.
- Riyadi, P. H., Romadhon, Sari, I. D., Kurniasih, R. A., Agustini, T. W., Swastawati, F., Herawati, V. E., & Tanod, W. A. (2021). SwissADME predictions of pharmacokinetics and drug-likeness properties of small molecules present in Spirulina platensis. *IOP Conference Series: Earth and Environmental Science*, *890*(1), 2063–2073. https://doi.org/10.1088/1755-1315/890/1/012021
- Roos, K., Wu, C., Damm, W., Reboul, M., Stevenson, J. M., Lu, C., Dahlgren, M. K., Mondal,
- S., Chen, W., Wang, L., Abel, R., Friesner, R. A., & Harder, E. D. (2019). OPLS3e: Extending Force Field Coverage for Drug-Like Small Molecules. *Journal of Chemical Theory and Computation*, *15*(3), 1863–1874. https://doi.org/10.1021/acs.jctc.8b01026
- Saab, Y. B., Kabbara, W., Chbib, C., & Gard, P. R. (2007). Buccal cell DNA extraction: Yield, purity, and cost: A comparison of two methods. *Genetic Testing*, *11*(4), 413–416. https://doi.org/10.1089/gte.2007.0044
- Sahoo, P. K., Das, L. M., Babu, M. K. G., & Naik, S. N. (2007). Biodiesel development from high acid value polanga seed oil and performance evaluation in a CI engine. *Fuel*, *86*(3), 448–454.

- Sathyadevi, P., Krishnamoorthy, P., Butorac, R. R., Cowley, A. H., Bhuvanesh, N. S. P., & Dharmaraj, N. (2011). Effect of substitution and planarity of the ligand on DNA/BSA interaction, free radical scavenging and cytotoxicity of diamagnetic Ni (II) complexes: a systematic investigation. *Dalton Transactions*, *40*(38), 9690–9702.
- Savage, D., Neary, N., Malone, G., Alley, S. R., Gallagher, J. F., & Kenny, P. T. M. (2005). The synthesis and structural characterization of novel N-meta-ferrocenyl benzoyl amino acid esters. *Inorganic Chemistry Communications*, *8*(5), 429–432.
- Schöppler, F., Mann, C., Hain, T. C., Neubauer, F. M., Privitera, G., Bonaccorso, F., Chu, D., Ferrari, A. C., & Hertel, T. (2011). Molar extinction coefficient of single-wall carbon nanotubes. *Journal of Physical Chemistry C*, *115*(30), 14682–14686. https://doi.org/10.1021/jp205289h
- Schreiner, W., Karch, R., Knapp, B., & Ilieva, N. (2012). Relaxation estimation of RMSD in molecular dynamics immunosimulations. *Computational and Mathematical Methods in Medicine*, *2012*. https://doi.org/10.1155/2012/173521
- Schrödinger. (2015). Small-Molecule Drug Discovery Suite 2015-3: Schrödinger Suite 2015-3 Induced Fit Docking protocol; Glide version 6.8; Prime version 4.1. *Glide Version*, *6*.
- Schrödinger. (2024). *Schrödinger Release 2024-1: LigPrep, Schrödinger, LLC.*
- Sellami, I. H., Maamouri, E., Chahed, T., Wannes, W. A., Kchouk, M. E., & Marzouk, B. (2009). Effect of growth stage on the content and composition of the essential oil and phenolic fraction of sweet marjoram (Origanum majorana L.). *Industrial Crops and Products*, *30*(3), 395–402.
- Shah, A., Zaheer, M., Qureshi, R., Akhter, Z., & Nazar, M. F. (2010). Voltammetric and spectroscopic investigations of 4-nitrophenylferrocene interacting with DNA. *Spectrochimica Acta Part A: Molecular and Biomolecular Spectroscopy*, *75*(3), 1082–1087.
- Shahabadi, N., Kashanian, S., Mahdavi, M., & Sourinejad, N. (2011). DNA interaction and DNA cleavage studies of a new platinum (II) complex containing aliphatic and aromatic dinitrogen ligands. *Bioinorganic Chemistry and Applications*, *2011*.
- Shamma, M. (1972). The Isoquinoline Alkaloids, New York and London. *Academic Press*, *81*, 335–341.
- Singh, S. (2002). Refractive index measurement and its applications. *Physica Scrip-*

ta, *65*(2), 167.

- Sliwoski, G., Kothiwale, S., Meiler, J., & Lowe, E. W. (2014). Computational methods in drug discovery. *Pharmacological Reviews*, *66*(1), 334–395.
- Telfer, E., Graham, N., Stanbra, L., Manley, T., & Wilcox, P. (2013). Extraction of high purity genomic DNA from pine for use in a high-throughput genotyping platform. *New Zealand Journal of Forestry Science*, *43*(1), 1–8. https://doi.org/10.1186/1179-5395-43-3
- Topală, T., Bodoki, A., Oprean, L., & Oprean, R. (2014). Bovine serum albumin interactions with metal complexes. *Clujul Medical*, *87*(4), 215.
- Tu, T., Rendleman, C. A., Borhani, D. W., Dror, R. O., Gullingsrud, J., Jensen, M. O., Klepeis,
- J. L., Maragakis, P., Miller, P., Stafford, K. A., & Shaw, D. E. (2008). A scalable parallel framework for analyzing terascale molecular dynamics simulation trajectories. *2008 SC - International Conference for High Performance Computing, Networking, Storage and Analysis, SC 2008*, 1–12. https://doi.org/10.1109/SC.2008.5214715
- Valarezo, E., Rosales, J., Morocho, V., Cartuche, L., Guaya, D., Ojeda-Riascos, S., Armijos, C., & González, S. (2015). Chemical composition and biological activity of the essential oil of Baccharis obtusifolia Kunth from Loja, Ecuador. *Journal of Essential Oil Research*, *27*(3), 212–216.
- Vera, R. R., & Chane-Ming, J. (1999). Chemical composition of the essential oil of marjoram (Origanum majorana L.) from Reunion Island. *Food Chemistry*, *66*(2),143–145.
- W., A. P. (1998). Physical Chemistry, 6th edition. Oxford University Press. *Chem. Soc. Rev.*, *41*(2), 753. http://xlink.rsc.org/?DOI=C1CS15191F
- Wang, E., Fu, W., Jiang, D., Sun, H., Wang, J., Zhang, X., Weng, G., Liu, H., Tao, P., & Hou, T. (2021). VAD-MM/GBSA: a variable atomic dielectric MM/GBSA model for improved accuracy in protein–ligand binding free energy calculations. *Journal of Chemical Information and Modeling*, *61*(6), 2844–2856.
- Wang, R., Fu, Y., & Lai, L. (1997). A new atom-additive method for calculating partition coefficients. *Journal of Chemical Information and Computer Sciences*, *37*(3), 615–621.
- Whitlock, R., Hipperson, H., Mannarelli, M., & Burke, T. (2008). A high-

throughput protocol for extracting high-purity genomic DNA from plants and animals. *Molecular Ecology Resources*, *8*(4), 736–741. https://doi.org/10.1111/j.1755-0998.2007.02074.x

- Yang, Y., Yao, K., Repasky, M. P., Leswing, K., Abel, R., Shoichet, B. K., & Jerome, S. V. (2021). Efficient exploration of chemical space with docking and deep learning. *Journal of Chemical Theory and Computation*, *17*(11), 7106–7119.
- Zhao, G.-C., Zhu, J.-J., Zhang, J.-J., & Chen, H.-Y. (1999). Voltammetric studies of the interaction of methylene blue with DNA by means of β-cyclodextrin. *Analytica Chimica Acta*, *394*(2–3), 337–37